iScience

Article

# Leveraging Vγ9Vδ2 T cells against prostate cancer through a VHH-based PSMA-Vδ2 bispecific T cell engager

## Graphical abstract

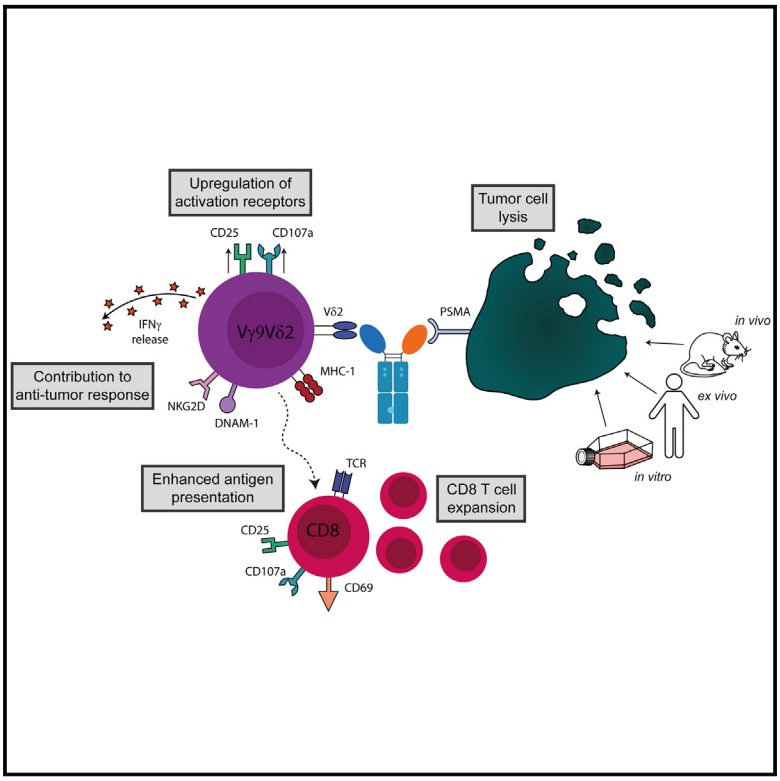


## Authors

Lisa A. King, Myrthe Veth, Victoria Iglesias-Guimarais, ..., Pauline M. van Helden, Tanja D. de Gruijl, Hans J. van der Vliet

## Correspondence

l.king@amsterdamumc.nl (L.A.K.), jj.vandervliet@amsterdamumc.nl (H.J.v.d.V.)

## In brief

Therapy; Immune response; Cancer

## Highlights

- PSMA-Vδ2 bsTCE-activated Vγ9Vδ2 T cells lyse prostate tumor cells while sparing normal cells
- PSMA-Vδ2 bsTCE-activated Vγ9Vδ2 T cells enhance antigen cross-presentation to $CD8^+$ T cells
- DNAM-1 and NKG2D contribute to Vγ9Vδ2 T cell activation at low PSMA-Vδ2 bsTCE concentrations
- Anti-tumor efficacy of PSMA-Vδ2 bsTCE was confirmed in *in vivo* immunodeficient NCG mice

King et al., 2024, iScience *27*, 111289
December 20, 2024 © 2024 The Authors. Published by Elsevier Inc.
https://doi.org/10.1016/j.isci.2024.111289

CellPress

iScience

CellPress
OPEN ACCESS

Article

# Leveraging Vγ9Vδ2 T cells against prostate cancer through a VHH-based PSMA-Vδ2 bispecific T cell engager

Lisa A. King,[1,2,3,9,*] Myrthe Veth,[1,2,3] Victoria Iglesias-Guimarais,[4] Iris Blijdorp,[4] Jan Kloosterman,[1,2,3] André N. Vis,[5,6] Rob C. Roovers,[4] David Lutje Hulsik,[4,8] Thilo Riedl,[4] Anton E.P. Adang,[4] Paul W.H.I. Parren,[4,7,8] Pauline M. van Helden,[4] Tanja D. de Gruijl,[1,2,3] and Hans J. van der Vliet[1,2,4,*]

[1]Department of Medical Oncology, Amsterdam UMC, Vrije Universiteit Amsterdam, Amsterdam 1081 HV, the Netherlands
[2]Cancer Center Amsterdam, 1081 HV Amsterdam, the Netherlands
[3]Amsterdam Institute for Infection and Immunity, Amsterdam, the Netherlands
[4]Lava Therapeutics NV, 3584 CM Utrecht, the Netherlands
[5]Prostate Cancer Network the Netherlands, Amsterdam, the Netherlands
[6]Department of Urology, Amsterdam UMC, Vrije Universiteit Amsterdam, HV Amsterdam 1081, the Netherlands
[7]Department of Immunology, Leiden University Medical Center, 2333 ZA Leiden, the Netherlands
[8]Present address: Gyes BV, 3584 CM Utrecht, the Netherlands
[9]Lead contact
*Correspondence: l.king@amsterdamumc.nl (L.A.K.), jj.vandervliet@amsterdamumc.nl (H.J.v.d.V.)
https://doi.org/10.1016/j.isci.2024.111289

## SUMMARY

Vγ9Vδ2 T cells constitute a homogeneous effector T cell population that lyses tumors of different origin, including the prostate. We generated a bispecific T cell engager (bsTCE) to direct Vγ9Vδ2 T cells to PSMA$^+$ prostate cancer (PCa) cells. The PSMA-Vδ2 bsTCE triggered healthy donor and PCa patient-derived Vγ9Vδ2 T cells to lyse PSMA$^+$ PCa cell lines and patient-derived tumor cells while sparing normal prostate cells and enhanced Vγ9Vδ2 T cell antigen cross-presentation to CD8$^+$ T cells. Vγ9Vδ2 T cell expressed NKG2D and DNAM-1 contributed to Vγ9Vδ2 T cell activation and tumor lysis at low PSMA-Vδ2 bsTCE concentrations. *In vivo* models confirmed the antitumor efficacy of the bsTCE and demonstrated a half-life of 6–7 days. Tissue-cross reactivity analysis was in line with known tissue distribution of PSMA and Vγ9Vδ2 T cells. Together these data show the PSMA-Vδ2 bsTCE to represent a promising anti-tumor strategy and supports its ongoing evaluation in a phase 1/2a clinical trial in therapy refractory metastatic castration-resistant PCa.

## INTRODUCTION

Prostate cancer (PCa) is the second most common cancer among men worldwide.[1] Initially, patients with metastatic PCa typically receive androgen-deprivation therapy (ADT).[2–4] When PCa becomes resistant to ADT (i.e., castration resistant), therapeutic approaches may include 2$^{nd}$ generation anti-hormonal agents (e.g., enzalutamide and abiraterone), chemotherapy (e.g., docetaxel and cabazitaxel), poly ADP-ribose polymerase inhibitors (e.g., olaparib and rucaparib), and most recently lutetium-177-prostate-specific membrane antigen (PSMA)-617 radioligand therapy.[5–7] Nevertheless, a high unmet medical need remains for patients with castration-resistant prostate cancer that do not benefit from these existing treatments long term.[5,8]

Immunotherapeutic strategies have demonstrated impressive improvements in treatment outcomes for multiple cancers, particularly in melanoma, non-small-cell lung carcinoma, and renal cell carcinoma. To date, anti-PD-1 monoclonal antibodies have been approved for only a fraction of PCa patients with high microsatellite instability (MSI-H) or mismatch repair deficient (dMMR) tumors.[9] Unfortunately, the overall efficacy of immunotherapy in PCa has been disappointing. This may be related to PCa, especially in advanced stages, being an immunologically cold tumor with an immunosuppressive tumor microenvironment enriched for Th17 cells, regulatory T cells (Tregs), and suppressive myeloid cell populations.[10–13] Whereas infiltration of conventional αβ T cells is generally limited in PCa, the frequency of tumor-infiltrating Vγ9Vδ2 T cells was reported to be relatively high in prostate tumors compared to other tumor types, with their abundance correlating with favorable outcome.[14] Vγ9Vδ2 T cells are activated by conformational changes in the butyrophilin (BTN) 2A1-BTN3A1 complex caused by intracellular binding of (non-peptidic) phosphoantigens, which accumulate in tumor cells through dysregulation of the mevalonate pathway.[15,16] Vγ9Vδ2 T cells can bridge innate and adaptive immune responses and harbor direct and indirect anti-tumor properties in an HLA-independent manner.[17,18] Activation of these cells


This is an open access article under the CC BY-NC-ND license (http://creativecommons.org/licenses/by-nc-nd/4.0/).

leads to secretion of pro-inflammatory cytokines (i.e., tumor necrosis factor [TNF] and interferon gamma [IFN-γ]), expansion, antigen presentation, recruitment of αβ T cells, and tumor lysis via perforin/granzyme B and Fas ligand.[19–24]

PSMA has been recognized as an attractive target in prostate cancer due to overexpression of the protein in the primary tumor, in cancerous lymph nodes and bone metastases, compared to non-malignant (healthy) prostate tissue.[25,26] Here, we set out to generate and characterize a PSMA-Vδ2 bispecific T cell engager (bsTCE) to direct the antitumor properties of Vγ9Vδ2 T cells to PCa. The PSMA-Vδ2 bsTCE effectively triggered Vγ9Vδ2 T cells to lyse multiple PSMA-expressing prostate tumors, but not non-malignant prostate tissue, inhibited tumor growth in an *in vivo* mouse model, and enhanced (tumor-associated) antigen cross-presentation to $CD8^+$ T cells. Tissue-cross reactivity studies confirmed binding to be restricted to tissues known to express PSMA or contain Vγ9Vδ2 T cells further supporting clinical evaluation of this Vγ9Vδ2 T cell targeted immunotherapy approach in PCa patients.

## RESULTS

### PSMA-Vδ2 bsTCEs bind to PSMA and Vδ2 and trigger Vγ9Vδ2 T cell degranulation and lysis of $PSMA^+$ tumor cells

To generate Vγ9Vδ2 T cell engagers, the PSMA-specific variable heavy domain of heavy chain (VHH) D2[27] was N-terminally (PSMA-Vδ2 bsTCE) or C-terminally (Vδ2-PSMA bsTCE) linked to the Vδ2-TCR-specific VHH5C8.[28] While both orientations of the bsTCE bound with similar half maximal effective concentration ($EC_{50}$) to Vγ9Vδ2 T cells (PSMA-Vδ2: 1.10 nM versus Vδ2-PSMA: 0.59 nM) (Figure 1A), a difference was observed in the $EC_{50}$ for binding to the $PSMA^+$ cell line LNCaP (PSMA-Vδ2: 14.12 nM versus Vδ2-PSMA: 65.37 nM, Figure 1B). No binding to PC3 tumor cells, which lack PSMA expression, was observed. In the presence of LNCaP cells both orientations of the bsTCE induced comparable Vγ9Vδ2 T cell degranulation, CD25 upregulation, IFN-γ production, and lysis of LNCaP cells (see Figures 1C and 1D, also for $EC_{50}$ values). Vγ9Vδ2 T cell degranulation, CD25 upregulation, IFN-γ production, and target cell lysis were not observed in co-cultures with $PSMA^-$ PC3 tumor cells, confirming target specificity. To facilitate clinical applicability, the PSMA-Vδ2 bsTCE was humanized using complementarity-determining region (CDR) grafting technology as described in the Star Methods section, and its binding to Vδ2 and PSMA was confirmed (Figure S2). In addition, as the expected plasma half-life of a bispecific VHH is short, the humanized bsTCE was produced with an Fc tail by linking the individual VHHs via a modified hinge to a human CH2 and CH3 domain (hereafter referred to as PSMA-Vδ2-Fc bsTCE; both humanized molecules are illustrated in Figure S1) to prolong plasma half-life. The PSMA-Vδ2-Fc bsTCE was shown to bind with (low) nM apparent affinity to Vγ9Vδ2 T cells ($EC_{50}$ 1.17 nM) and LNCaP cells ($EC_{50}$ 18.42 nM) (Figure 2A) similarly to the bsTCE without Fc tail. Activation of Vγ9Vδ2 T cells was observed in co-cultures with several PSMA-expressing tumor cell lines i.e., 22Rv1, VCaP (Figure 2B), and LNCaP in the presence of the PSMA-Vδ2-Fc bsTCE as shown by the induction of degranulation, CD25 upregulation, and IFN-γ production (Figure 2C, with all listed $EC_{50}$ values). All three $PSMA^+$ tumor cell lines were efficiently lysed by Vγ9Vδ2 T cells in a bsTCE concentration-dependent manner (Figure 2D). No binding of the PSMA-Vδ2-Fc bsTCE to LNCaP PSMA knockout cells or PC3 cells was detected (Figure 2A), and Vγ9Vδ2 T cells did not degranulate when exposed to LNCaP PSMA KO cells or PC3 cells (Figure 2C), nor were PC3 cells lysed in the presence of the bsTCE (Figure 2D). Control bsTCEs did not bind to Vγ9Vδ2 T cells nor LNCaP cells (Figure 2A) and did not induce Vγ9Vδ2 T cell activation or tumor cell lysis (Figure 2E).

These data demonstrate that both bispecific VHHs with or without the Fc domain bind Vγ9Vδ2 T cells and $PSMA^+$ tumor cells similarly and trigger target-dependent and specific Vγ9Vδ2 T cell activation, degranulation, cytokine release, and lysis of $PSMA^+$ prostate tumor cells at sub-nanomolar concentrations.

### PSMA-Vδ2-Fc bsTCE triggers activation of Vγ9Vδ2 T cells in prostate cancer patient-derived tumor tissue and PBMC and induces selective prostate tumor cell lysis

We next assessed the frequency and phenotype of Vγ9Vδ2 T cells in PCa patient-derived peripheral blood mononuclear cell (PBMC) and malignant and non-malignant prostate tissue suspensions and tested their activation in the presence of the bsTCE. As shown in Figure 3A, the frequency of Vγ9Vδ2 T cells (of total $CD3^+$ T cells) was 2.6 ± 0.7% (mean ± SEM; $n$ = 40) in PBMC, 1.4 ± 0.4% (mean ± SEM; $n$ = 31) in non-malignant prostate tissue and 1.6 ± 0.5% (mean ± SEM; $n$ = 31) in malignant prostate tissue. Phenotypic analysis of Vγ9Vδ2 T cells and $CD3^+$ non-Vγ9Vδ2 T cells (T cells) is shown in Figure 3B. Expression of the early activation and tissue-residency marker CD69 was observed on the majority of Vγ9Vδ2 T cells with a non-significant trend toward more cells expressing CD69 in non-malignant and malignant prostate tissue compared to PBMC (CD69 mean ± SEM: 81.4% ± 8.9% of Vγ9Vδ2 T cells in non-malignant; 87.7% ± 6.0% of Vγ9Vδ2 T cells in malignant prostate tissue; 68.1% ± 4.5% of Vγ9Vδ2 T cells in PBMC). Vγ9Vδ2 T cell expression of the co-stimulatory molecule 4-1BB, typically expressed on activated T cells, was generally limited and mostly restricted to cells in malignant prostate tissue. Malignant prostate tissue also contained the highest frequency of Vγ9Vδ2 T cells expressing the terminal differentiation marker CD57. Expression levels of the PD-1 immune checkpoint receptor did not statistically differ between Vγ9Vδ2 T cells from PBMC and prostate tissue. While the percentage of $CD3^+$ cells expressing 4-1BB was higher in malignant prostate tissue, expression of CD69 and PD-1 was significantly higher in both non-malignant and malignant prostate tissue compared to PBMC. Expression of CD57 on $CD3^+$ cells was not different in PBMC or prostate tissue. In order to explore the functional responsiveness of Vγ9Vδ2 T cells in PCa patients to PSMA-Vδ2-Fc bsTCE, we tested Vγ9Vδ2 T cell degranulation and tumor cell lysis in cultures of non-malignant (PSMA expression MFI mean ± SEM; 0.7 ± 0.3) and malignant (PSMA expression MFI mean ± SEM; 5.7 ± 2.4) prostate tissue alone or in co-cultures with autologous patient-derived PBMC added. In the case of malignant prostate tissue, addition of the PSMA-Vδ2-Fc bsTCE resulted in a significant increase in degranulation of both tissue infiltrated (TI; 4 h co-cultures, $p$ =

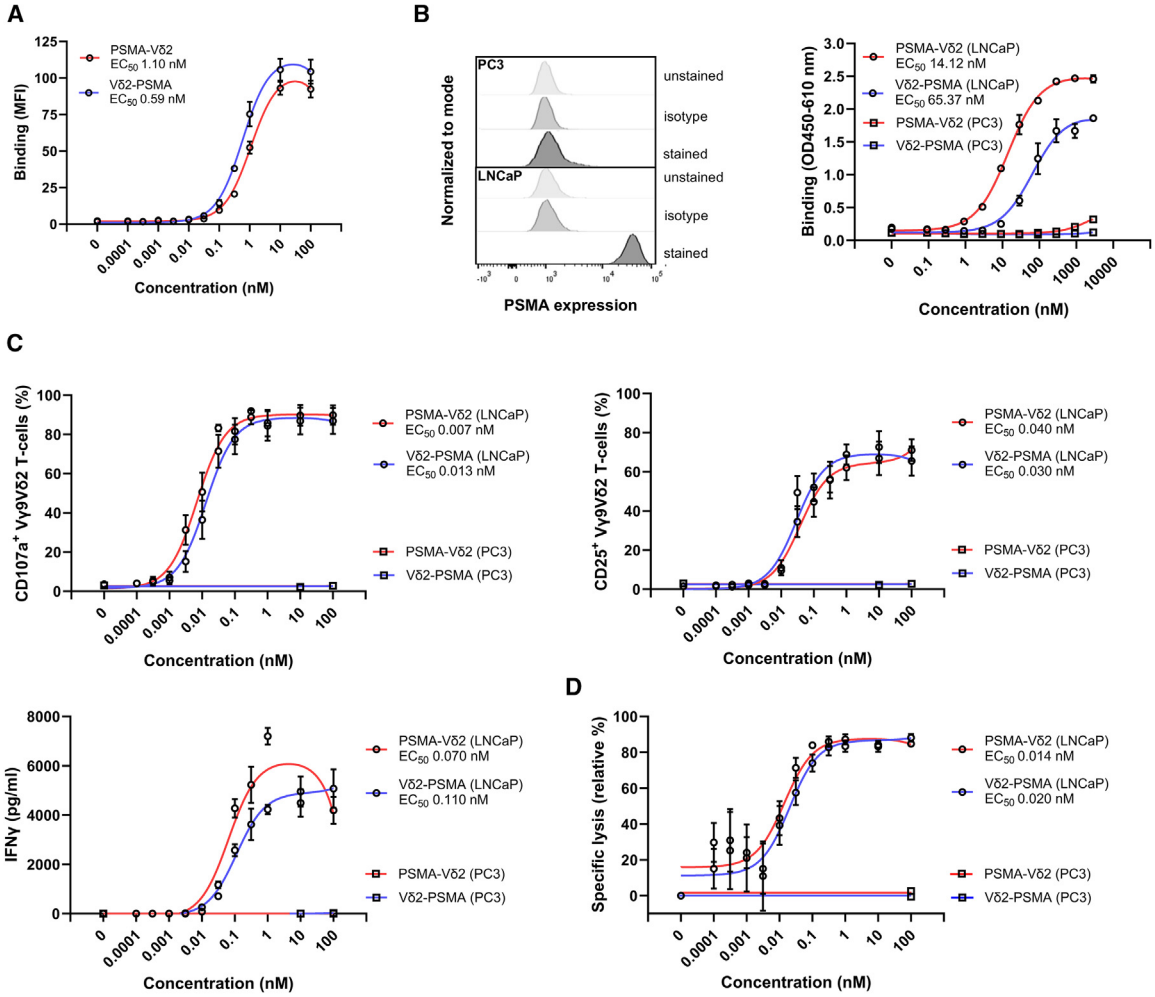


**Figure 1. Impact of binding domain order in PSMA-Vδ2 bsTCEs on cell binding and induction of cytolytic activity of Vγ9Vδ2 T cells**

(A) Binding of non-humanized PSMA-Vδ2 and Vδ2-PSMA bsTCE to expanded Vγ9Vδ2 T cells ($n = 7$).

(B) PSMA expression shown as histogram ($n = 1$) and binding of non-humanized bsTCEs to LNCaP ($n = 2$) and PC3 cells ($n = 2$).

(C) Vγ9Vδ2 T cell CD107a expression ($n = 5$), CD25 expression ($n = 3$), IFN-γ secretion ($n = 3$).

(D) Target cell lysis ($n = 5$) in 24 h co-cultures of expanded Vγ9Vδ2 T cells with LNCaP or PC3 with indicated concentrations of non-humanized bsTCEs. Data were generated using flow cytometry (A, B left, C CD107a and CD25, D), ELISA (B right) or CBA (C IFNγ). Data represent mean ± S.E.M.

0.005) and peripheral blood Vγ9Vδ2 T cells (24 h co-cultures, $p = 0.04$) (Figure 3C). In contrast, the PSMA-Vδ2-Fc bsTCE did not enhance degranulation of Vγ9Vδ2 T cells when added to non-malignant prostate tissue (containing autologous TI lymphocytes) alone or to co-cultures containing non-malignant prostate tissue and autologous PBMC (Figure 3D). Lysis of prostate tumor cells (defined as $CD45^{-}EpCAM^{dim/+}$ cells) and non-malignant prostate cells (defined as $CD45^{-}EpCAM^{-}$ cells) was also assessed. In 24 h co-cultures with autologous PCa patient-derived PBMC (PBMC:target cell ratio = 10:1; Vγ9Vδ2 T cell:target cell ratio = 1:25 [donor 1], 1:9 [donor 2], and 1:5 [donor 3]), we observed lysis of prostate tumor cells triggered by the PSMA-Vδ2-Fc bsTCE, whereas non-malignant prostate cells were spared (Figure 3E). Of note, in 2/3 donors, tumor lysis was also observed in the PSMA-Vδ2-Fc bsTCE only conditions and therefore mediated by intratumoral Vγ9Vδ2 T cells.

## NKG2D and DNAM-1 receptor interactions contribute to PSMA-Vδ2-Fc bsTCE-induced Vγ9Vδ2 T cell degranulation and tumor cell lysis at functionally non-saturating bsTCE concentrations

Expression levels of PSMA and of co-stimulatory and co-inhibitory ligands were determined on malignant and non-malignant prostate tissue to assess their possible contribution to the observed tumor specificity of Vγ9Vδ2 T cells upon binding of the PSMA-Vδ2-Fc bsTCE. As expected, prostate cancer cells expressed significantly higher levels of PSMA compared to non-malignant prostate cells ($p \leq 0.0001$; Figure 4A). This was further confirmed using paired non-malignant and malignant tissue samples from 30 PCa patients ($p \leq 0.0001$; Figure 4B). We also observed BTN3A and BTN2A1, receptors critically involved in mediating the phosphoantigen dependent activation of Vγ9Vδ2 T cells, to be expressed at significantly higher levels

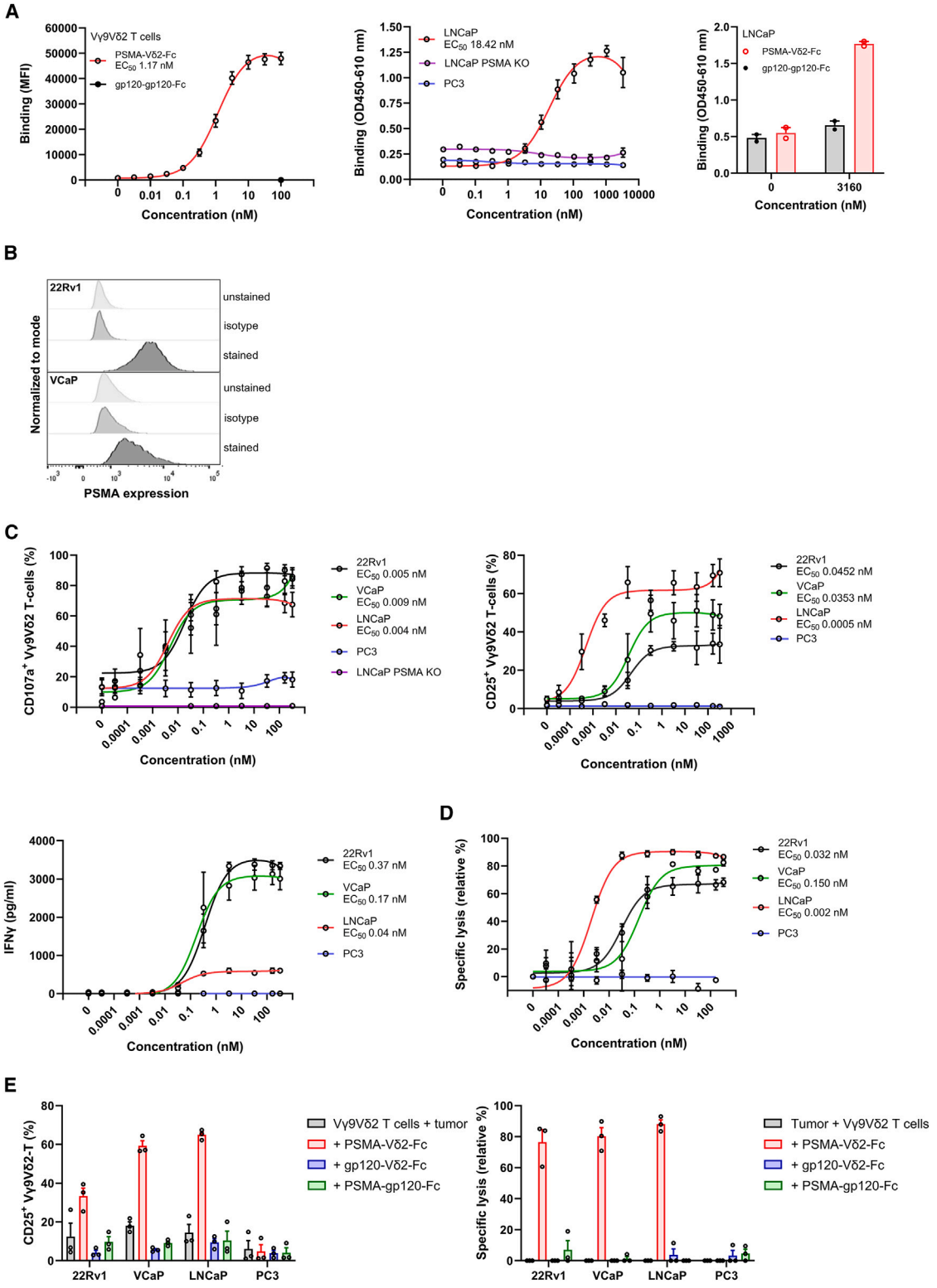


**Figure 2. Target binding, Vγ9Vδ2 T cell activation, and tumor cell lysis by the PSMA-Vδ2-Fc bsTCE**

(A) PSMA-Vδ2-Fc bsTCE and control bsTCE binding to expanded Vγ9Vδ2 T cells ($n$ = 6), LNCaP (left: $n$ = 3, right: $n$ = 2), and PC3 cells ($n$ = 1).

(B) PSMA expression by 22Rv1 and VCaP shown as histograms.

*(legend continued on next page)*

on malignant versus non-malignant prostate cells ($p \leq 0.0001$ and $p = 0.04$, respectively Figure 4C). Similarly, the Vγ9Vδ2 T cell activating ligands nectin-2 and poliovirus receptor (PVR) (DNAM-1 ligands) as well as MIC-A/B, ULBP-3, and ULBP-2/5/6 (NKG2D ligands) were found to be expressed at significantly higher levels by malignant versus non-malignant prostate cells (nectin-2: $p = 0.003$, PVR: $p = 0.01$, MIC-A/B: $p = 0.003$, ULBP-3: $p = 0.02$ and ULBP-2/5/6: $p = 0.03$; Figures 4D and 4E). Only the NKG2D ligand ULBP-1 was expressed at similar levels ($p = 0.2$; Figure 4E). Also, HLA-E, the ligand for the inhibitory NKG2A receptor was expressed at significantly higher levels on malignant prostate cells compared to non-malignant prostate cells ($P$=<0.0001; Figure 4F). Frequencies of Vγ9Vδ2 T cells that expressed the receptors for these ligands, DNAM-1, NKG2D, and NKG2A, varied substantially between patients and were not statistically significantly different between Vγ9Vδ2 T cells in PBMC, non-malignant or malignant prostate tissue in the case of NKG2D and NKG2A (Figure 4G). The frequency of DNAM-1 expressing Vγ9Vδ2 T cells was lower in malignant tissue (PBMC versus malignant $p \leq 0.0001$, non-malignant versus malignant $p = 0.03$), though the intensity of expression (in MFI) on DNAM-1 expressing Vγ9Vδ2 T cells was very similar between groups.

Following the observation of higher levels of BTN3A, BTN2A1, and ligands of NKG2D, NKG2A, and DNAM-1 on prostate tumor cells, we next assessed whether receptor interactions involving these molecules could contribute to Vγ9Vδ2 T cell reactivity induced by the PSMA-Vδ2-Fc bsTCE, using monoclonal antibodies blocking these interactions. For this purpose healthy donor derived expanded DNAM-1, NKG2D, and NKG2A expressing Vγ9Vδ2 T cells were co-cultured with either of three prostate cancer cell lines expressing variable levels of PSMA, BTN3A, and DNAM-1, NKG2D, and NKG2A ligands (expression of DNAM-1, NKG2D, and NKG2A on Vγ9Vδ2 T cells is shown in Figure S3A and expression of BTN3A and DNAM-1, NKG2D and NKG2A ligands shown in Figure S3B) in the absence or presence of PSMA-Vδ2-Fc bsTCE concentrations that, based on experiments shown in Figure 2, triggered maximal (5 nM) or sub-optimal (1 pM and 5 pM) Vγ9Vδ2 T cell activation and cytotoxicity.

Vγ9Vδ2 T cell degranulation, cytokine production, and tumor cell lysis increased with increasing dose of PSMA-Vδ2-Fc bsTCE (Figures 5A and 5B; Figures S3 and S4). When functionally saturating concentrations of the PSMA-Vδ2-Fc bsTCE were used, Vγ9Vδ2 T cell degranulation and tumor lysis were strong regardless of the presence of neutralizing antibodies. In the absence of PSMA-Vδ2-Fc bsTCE or in the presence of non-saturating concentrations of PSMA-Vδ2-Fc bsTCE, DNAM-1 receptor-ligand interactions impacted Vγ9Vδ2 T cell reactivity to LNCaP, VCaP, and 22Rv1 cells, as degranulation was significantly reduced in the presence of the DNAM-1 blocking antibody (Figure 5A). Similar trends were observed when specific tumor cell lysis (Figure 5B) and Vγ9Vδ2 T cell cytokine production were assessed (Figure S4). The impact of blocking NKG2D receptor-ligand interactions on Vγ9Vδ2 T cell reactivity to PSMA-Vδ2-Fc bsTCE only reached statistical significance in the presence of LNCaP cells (Figures 5C and 5D which may be related to the higher NKG2D ligand expression levels on LNCaP compared to VCaP and 22Rv1 cells (Figure S3B). Vγ9Vδ2 T cell degranulation was not statistically significantly affected by the presence of either BTN3A or NKG2A neutralizing antibodies (Figure S5). To explore whether these receptor interactions also impacted Vγ9Vδ2 T cell reactivity in patient samples, we cultured prostate tumor sample single-cell suspensions of 3 patients in the presence of 0.05 nM PSMA-Vδ2-Fc bsTCE and either DNAM-1 or NKG2D blocking antibodies *ex vivo* for 4 h. The PSMA-Vδ2-Fc bsTCE induced increase in Vγ9Vδ2 T cell degranulation was significantly reduced in the presence of a DNAM-1 blocking antibody whereas the NKG2D blocking antibody only reduced degranulation in 1 of the 3 donors (Figure 5E). In line with this observation, the tumor-infiltrating Vγ9Vδ2 T cells of this patient expressed higher baseline NKG2D levels than the other 2 donors (MFI: 3.34 versus MFI: 1.52 and 1.66). In conclusion, DNAM-1 and NKG2D receptor interactions contribute to Vγ9Vδ2 T cell reactivity and prostate cancer lysis in the absence of or in the presence of functionally non-saturating PSMA-Vδ2-Fc bsTCE concentrations.

## Activation of Vγ9Vδ2 T cells by bsTCE enhances their capacity to function as antigen-presenting cells

It was reported that phosphoantigen-activated Vγ9Vδ2 T cells can function as antigen presenting cells (APCs) and can (cross-) present antigens to $CD4^+$ and $CD8^+$ T cells.[29–31] We therefore evaluated whether bsTCE-activated Vγ9Vδ2 T cells could also exert APC functions. When freshly isolated (non-expanded) Vγ9Vδ2 T cells were co-cultured for 24 h with PSMA-Vδ2 bsTCE in PSMA protein-coated plates, we observed a significant increase in expression of CD83, HLA-A2, and HLA-DR, which are known APC-associated ligands also expressed by mature dendritic cells[32] (Figure 6A). Next, to study the effect of bsTCE on peptide cross-presentation by Vγ9Vδ2 T cells, we selected 3 model long peptides (LP), derived from the influenza M1 protein, the cytomegalovirus (CMV) pp65 protein, and the melanoma associated MART-1 protein, that contain known sequences that can be recognized by anti-viral (M1 and pp65) and anti-tumor (MART-1) specific $CD8^+$ T cells. As these 25-30-mer LPs require intracellular processing and cross-presenting on HLA-A2 molecules in order to activate antigen specific $CD8^+$ T cells, the Vγ9Vδ2 T cells used for these experiments were derived from HLA-A2 positive donors. We observed that (expanded) Vγ9Vδ2 T cells that were pre-activated by the PSMA-Vδ2 bsTCE using PSMA-coated plates induced significantly more activation (expression of CD69, CD25, CD107a,

(C) Vγ9Vδ2 T cell CD107a expression, CD25 expression, and IFN-γ secretion ($n = 3$).
(D) Target cell lysis ($n = 3$–4) in 24 h co-cultures of expanded Vγ9Vδ2 T cells with 22Rv1, VCaP, LNCaP (WT or PSMA KO), or PC3 with indicated concentrations of bsTCE.
(E) Vγ9Vδ2 T cell CD25 expression ($n = 3$) and target cell lysis ($n = 3$) in 24 h co-cultures of expanded Vγ9Vδ2 T cells with 22Rv1, VCaP, LNCaP, or PC3 with 100 nM PSMA-Vδ2-Fc bsTCE or control bsTCEs. Data were generated using flow cytometry (A left, B, C; CD107a and CD25, D, E), ELISA (A, middle and right) or CBA (C, IFNγ). Data represent mean ± S.E.M.

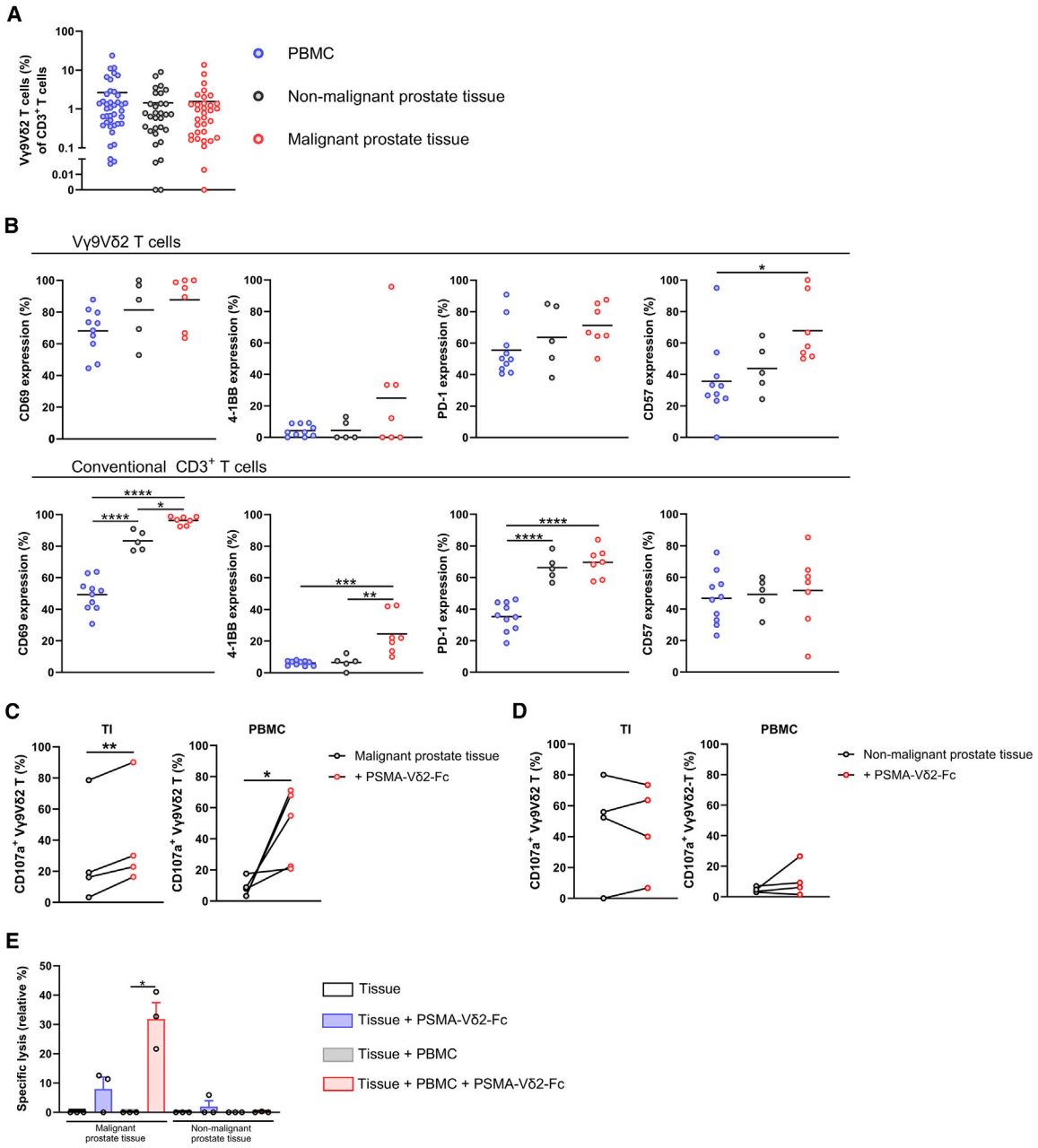


**Figure 3. PCa patient Vγ9Vδ2 T cell frequency, phenotype, and cytolytic activity in the presence of PSMA-Vδ2-Fc bsTCE**

(A) Vγ9Vδ2 T cell frequency (percentage of total T cells) in PBMC and non-malignant and malignant prostate tissue derived from PCa patients with primary prostate cancer.

(B) CD69, 4-1BB, PD-1, and CD57 expression (%) on Vγ9Vδ2 T cells or conventional $CD3^+$ T cells (non-Vγ9Vδ2 T cells).

(C) CD107a expression on Vγ9Vδ2 T cells within tissue infiltrate (TI) derived from malignant prostate tissue (4 h culture, $n = 4$) or CD107a expression on Vγ9Vδ2 T cells derived from autologous PBMC cultured with malignant prostate tissue (right, 24 h culture, 10:1 ratio, $n = 5$) with or without 50 nM PSMA-Vδ2-Fc bsTCE.

(D) CD107a expression on Vγ9Vδ2 T cells derived from non-malignant prostate tissue (left, 4 h culture, $n = 4$) or CD107a expression on Vγ9Vδ2 T cells derived from autologous PBMC cultured with non-malignant prostate tissue (right, 24 h culture, 10:1 ratio, $n = 4$) with or without 50 nM PSMA-Vδ2-Fc bsTCE.

(E) Target cell lysis of $CD45^-EpCAM^{dim/+}$ cells from malignant tissue ($n = 3$) or $CD45^-EpCAM^-$ cells derived from non-malignant tissue ($n = 3$) from patients with primary PCa in the presence or absence of matched PBMC in a 10:1 PBMC:tissue ratio after 24 h cultures. Data were generated using flow cytometry, circles represent individual patient samples and the mean (A and B) or mean ± S.E.M (E) are shown. One-way ANOVA with Dunnet multiple comparisons test (B), paired t test (C and E). $p < 0.05$: *, $p < 0.01$: **, $p < 0.001$: *** and $p < 0.0001$: ****.

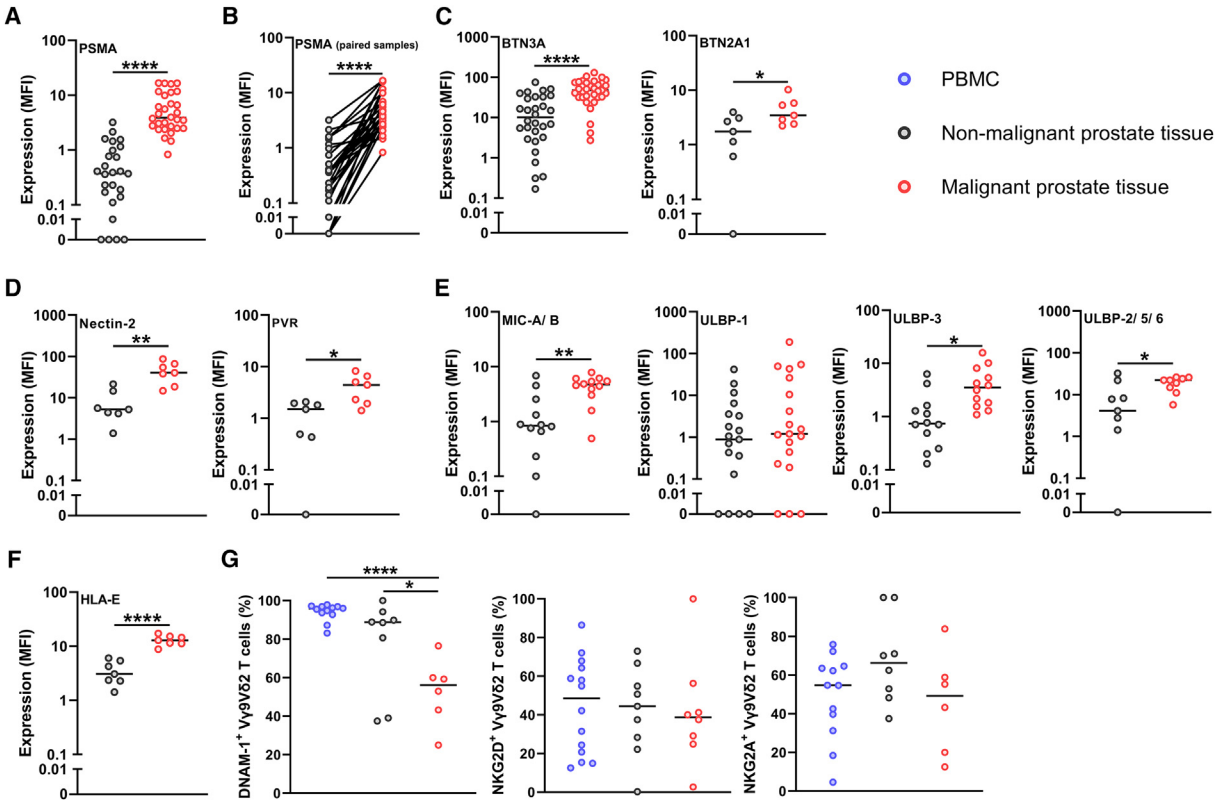


**Figure 4. Phenotypic analysis of ligands on PCa patient-derived tissue samples and matched co-receptors on PCa patient-derived Vγ9Vδ2 T cells**

(A–G) Expression levels (MFI or percentage) of PSMA, BTN3A, BTN2A1, nectin-2, PVR, MIC-A/B, ULBP-1, 2, 3, 5, HLA-E, DNAM-1, NKG2D, and NKG2A on PCa patient-derived tissue samples and Vγ9Vδ2 T cells. Individual patient samples are indicated using circles. Data were generated using flow cytometry and the median is shown. MFI = mean fluorescent intensity. Paired t test (A–F), one-way ANOVA with Dunnet multiple comparisons test (G). $p < 0.05$: *, $p < 0.01$: ** and $p < 0.0001$: ****.

and IFN-γ) of M1 or MART-1 specific CD8$^+$ T cells when pulsed with M1 or MART-1 LPs during the stimulation (Figures 6B and 6C). As illustrated in Figure 6D, a similar experiment was performed using freshly isolated (non-expanded) Vγ9Vδ2 T cells. Freshly isolated Vγ9Vδ2 T cells pre-activated with PSMA-Vδ2 bsTCE induced significantly more activation (CD69 and CD107a) of pp65-specific CD8$^+$ T cells when pulsed with pp65 LP during stimulation. We observed that pp65 LP cross-presentation by PSMA-Vδ2 bsTCE activated (expanded) Vγ9Vδ2 T cells also promoted an increase in the frequency of pp65-specific CD8$^+$ T cells among CD8$^+$ T cells from a CMV$^+$ donor (Figure 6E). This suggests an improved survival/proliferation of antigen-specific CD8$^+$ T cells by PSMA-Vδ2 bsTCE activated and pp65-loaded Vγ9Vδ2 T cells. To determine if those activated pp65-specific CD8$^+$ T cells were functional and could induce cytotoxicity of tumor cells, unloaded or pp65 short peptide (SP, not requiring antigen processing)-loaded THP-1 tumor cells were subsequently added as target cells to those cultures and incubated for another 24 h. As shown in Figure 6F, we observed that CD8$^+$ T cells co-cultured with pp65 LP pre-treated Vγ9Vδ2 T cells induced significantly more cytotoxicity of pp65 SP-loaded THP-1 tumor cells compared to CD8$^+$ T cells co-cultured with Vγ9Vδ2 T cells that were not exposed to pp65 LP. Tumor cell cytotoxicity was not seen when THP-1 tumor cells were not pre-loaded with pp65 SP, indicating that the observed lysis is specifically mediated via pp65-specific CD8$^+$ T cell recognition of the tumor cells (Figure 6F left panel).

## PSMA-Vδ2-Fc bsTCE triggers *in vivo* antitumor activity in a xenograft PCa model using human PBMC

In order to evaluate the *in vivo* therapeutic efficacy of the PSMA-Vδ2-Fc bsTCE, male immunodeficient NCG mice were inoculated subcutaneously with 22Rv1 tumor cells admixed with human healthy donor derived PBMC in a ratio of 2:1 (22Rv1:PBMC, $n$ = 2 PBMC donors: Vγ9Vδ2 T cell frequencies of respectively 21.9% and 8.8% of total CD3$^+$ cells resulting in 22Rv1:Vγ9Vδ2-T ratios of 22:1 and 60:1. Mice were treated with the PSMA-Vδ2-Fc bsTCE (0.2 and 2.0 mg/kg) or PBS intravenously weekly on day 0, 7, 14, and 21 starting at the day of tumor cell and PBMC inoculation and animals were sacrificed when the mean tumor volume of a group exceeded 2.000 mm$^3$. As shown in Figures 7A and 7B, inoculation of PBMC alone did not influence tumor growth but in combination with the PSMA-Vδ2-Fc bsTCE treatment (0.2 mg/kg and 2.0 mg/kg) led to significant tumor growth inhibition (0.2 mg/kg: $p \leq 0.0001$, TGI 61% and 2.0 mg/kg: $p \leq 0.0001$ and TGI 60% on day 37) resulting in a significant

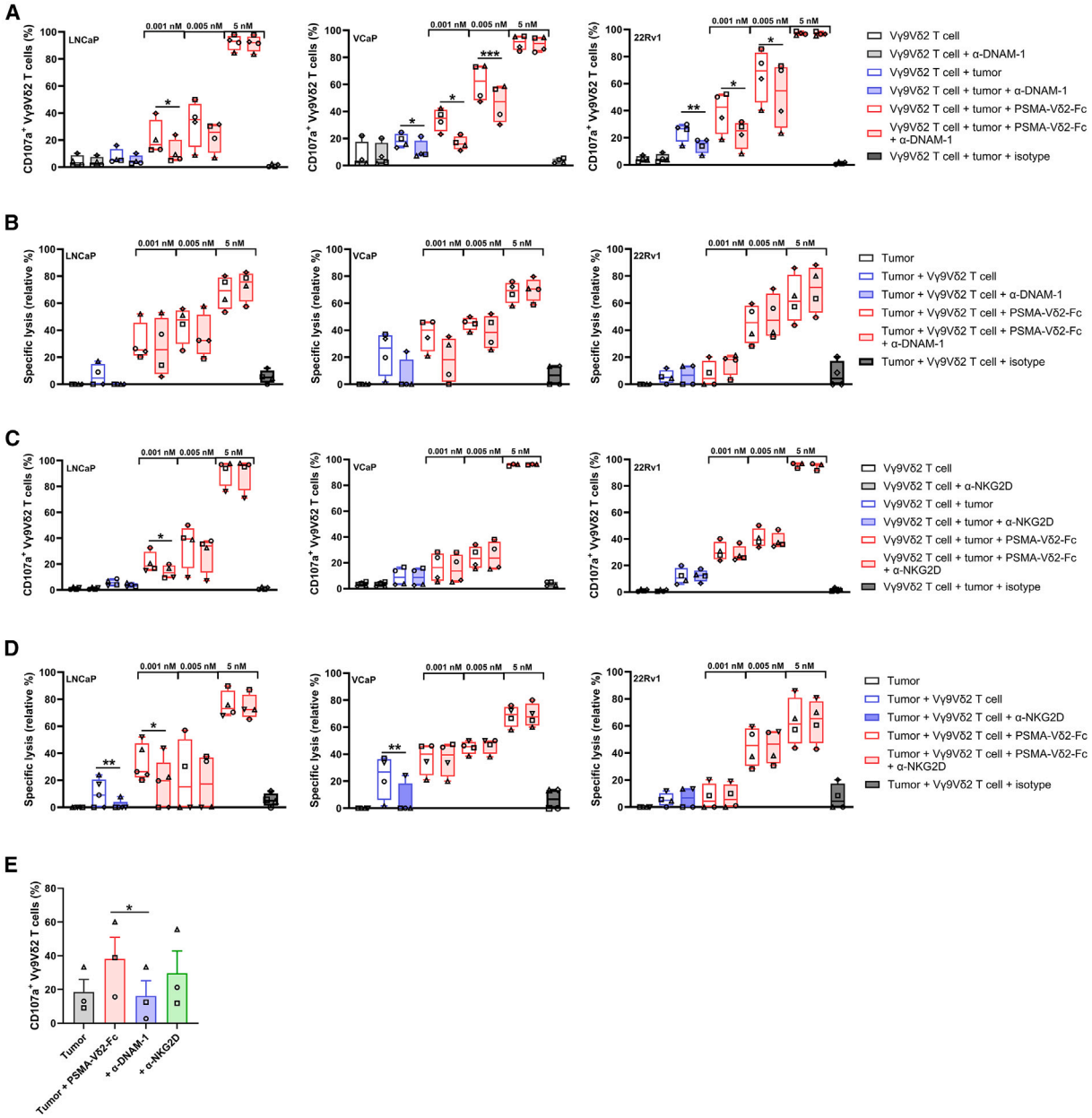


**Figure 5. Impact of DNAM-1 and NKG2D receptor interactions in PSMA-Vδ2-Fc bsTCE mediated Vγ9Vδ2 T cell activation and prostate tumor cell lysis**

(A) CD107a expression (4 h culture, $n = 4$) and (B) tumor cell lysis (24 h culture, $n = 4$) from cultures of expanded Vγ9Vδ2 T cells pre-incubated with 10 μg/mL anti-Fc receptor Ab and α-DNAM-1 blocking antibody or IgG1 isotype control with LNCaP, VCaP, or 22Rv1 tumor cells with indicated concentrations of PSMA-Vδ2-Fc bsTCE.

(C and D) (C) CD107a expression (4 h culture, $n = 4$) and (D) tumor cell lysis (24 h culture, $n = 4$) from cultures of expanded Vγ9Vδ2 T cells pre-incubated with 10 μg/mL anti-Fc receptor Ab and α-NKG2D blocking antibody or IgG1 isotype control with LNCaP, VCaP, or 22Rv1 tumor cells with indicated concentrations of PSMA-Vδ2-Fc bsTCE.

(E) CD107a expression on Vγ9Vδ2 T cells derived from malignant prostate tissue ($n = 3$) of PCa patients after 4 h co-culture with 0.05 nM PSMA-Vδ2-Fc bsTCE and α-DNAM-1 or α-NKG2D blocking Ab. Data were all generated using flow cytometry and circles represent individual data-points. Box and whisker plots indicate the median, 25th to 75th percentiles and minimum to maximum and bar graphs represent mean ± S.E.M. Paired t test (A, C–E). $p < 0.05$: *, $p < 0.01$: ** and $p < 0.001$: ***.

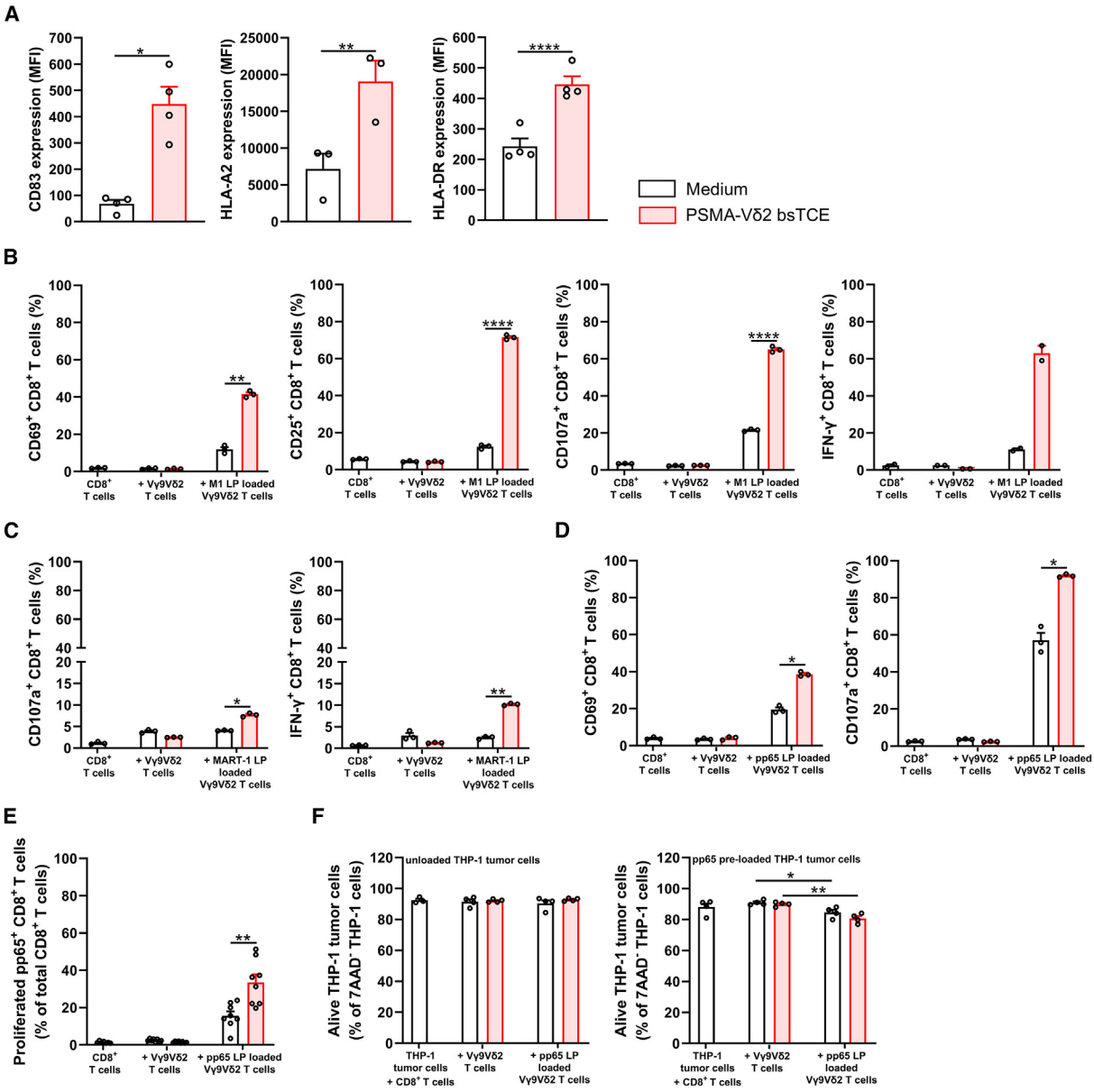


**Figure 6. Cross-presentation of virus-specific and tumor-associated antigens by PSMA-Vδ2 bsTCE activated Vγ9Vδ2 T cells**

(A) Expression of CD83, HLA-A2 and HLA-DR (MFI) by non-expanded Vγ9Vδ2 T cells ($n$ = 3–4) after 24 h incubation with 10 pM PSMA-Vδ2 bsTCE or medium on 1 μg/mL PSMA-coated plates.

(B–F) Vγ9Vδ2 T cells (expanded or non-expanded) were pre-incubated for 24 h with 10 pM PSMA-Vδ2 hu-bsTCE or medium with or without 1 μM M1, MART-1, or pp65 LPs on 1 μg/mL PSMA-coated plates and were subsequently incubated with M1, MART-1, or pp65-specific $CD8^+$ T cells. (B) Expression of CD69, CD25, CD107a, or IFN-γ (%) by M1-specific $CD8^+$ T cells incubated for 16–24 h with expanded Vγ9Vδ2 T cells as described. (C) Expression of CD107a and IFN-γ (%) by MART-1 specific $CD8^+$ T cells incubated 16–24 h with expanded Vγ9Vδ2 T cells as described. (D) Expression of CD69 and CD107a (%) by pp65-specific $CD8^+$ T cells incubated 16–24 h with non-expanded Vγ9Vδ2 T cells as described. (E) Percentage of pp65-specific $CD8^+$ T cells within $CD8^+$ T cell population ($CD8^+$ cells of $CMV^+$ healthy donor were used) incubated for 7 days with expanded Vγ9Vδ2 T cells as described. (F) Lysis of THP-1 tumor cells unloaded (left) or pre-loaded with 1 μM pp65 SP (right) after 24 h co-culture with $CD8^+$ T cell fractions that were variably enriched for pp65-specific cells during the 7 days co-culture with expanded Vγ9Vδ2 T cells as shown in (E). Live target cells were determined as % of $7AAD^-$ THP-1 cells. Data were all generated using flow cytometry, circles represent individual data-points and mean ± S.E.M. is shown. MFI = mean fluorescent intensity. Paired t test (A), two-way ANOVA with Tukey multiple comparisons test (B–E). $p < 0.05$: *, $p < 0.01$: ** and $p < 0.0001$: ****.

increase in overall survival (0.2 mg/kg: $p \leq 0.0001$ and 2.0 mg/kg: $p \leq 0.0001$) with a median overall survival of 49.5 days in the PSMA-Vδ2-Fc treated groups and 37 days in the PBS treated group. These data show that the PSMA-Vδ2-Fc bsTCE triggers *in vivo* antitumor activity using non-expanded freshly isolated PBMC.

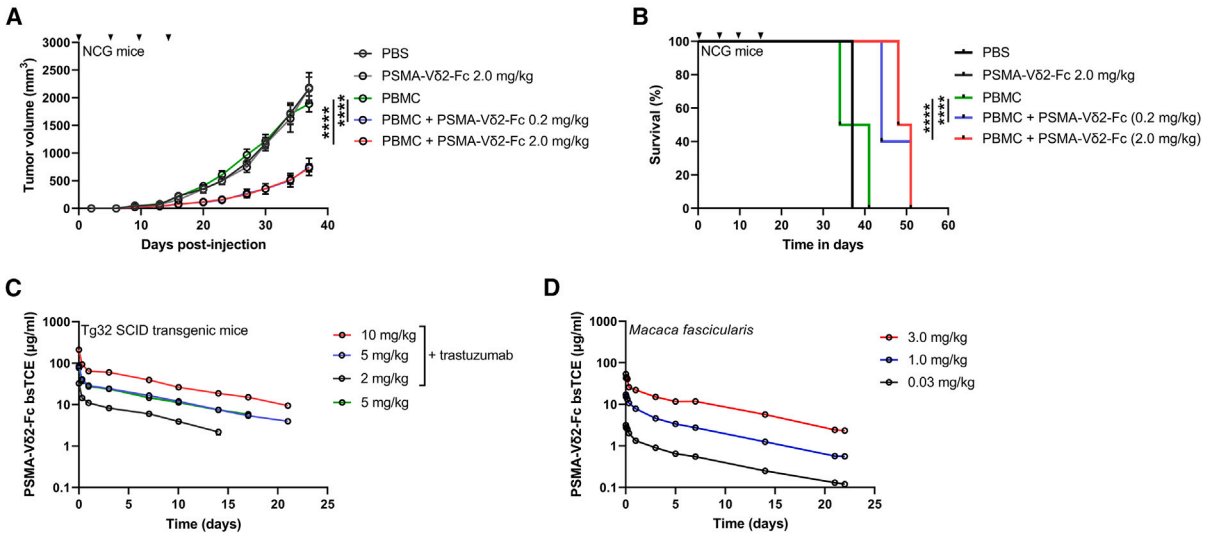


**Figure 7. *In vivo* anti-tumor activity and pharmacokinetics of PSMA-Vδ2-Fc bsTCE**

NCG mice were engrafted subcutaneously with 22Rv1 PSMA$^+$ tumor cells with or without PBMC and treated with PBS ($n$ = 4), 2.0 mg/kg PSMA-Vδ2-Fc bsTCE ($n$ = 4), PBMC ($n$ = 12), PBMC and 0.2 mg/kg PSMA-Vδ2-Fc bsTCE ($n$ = 12) or PBMC and 2.0 mg/kg PSMA-Vδ2-Fc bsTCE ($n$ = 12). PSMA-Vδ2-Fc bsTCE was administered weekly for four weeks.

(A) Tumor volume in mm$^3$.

(B) Survival curve.

(C) PSMA-Vδ2-Fc bsTCE plasma concentration (µg/mL) over time in Tg32 SCID transgenic mice injected intravenously with 2, 5, or 10 mg/mL PSMA-Vδ2-Fc bsTCE with ($n$ = 4) or without ($n$ = 3) 2, 5, or 10 mg/kg trastuzumab.

(D) PSMA-Vδ2-Fc bsTCE plasma concentration (µg/mL) over time in *Macaca fascicularis* injected with 0.03, 1.0, or 3.0 mg/kg PSMA-Vδ2-Fc bsTCE ($n$ = 1 per concentration). Black arrowheads indicate PSMA-Vδ2-Fc bsTCE injections. Data were generated by measuring tumor volume using a caliper (A) or ELISA (C and D) and represent mean ± S.E.M. Two-way ANOVA (A), mantel-cox test (B). $p < 0.0001$: ****.

## Pharmacokinetics of PSMA-Vδ2-Fc bsTCE in human FcRn-transgenic mice and non-human primates

Pharmacokinetic properties of the PSMA-Vδ2-Fc bsTCE were assessed in two *in vivo* animal models using animal species with no cross-reactivity with the bsTCE, i.e., mice and non-human primates. In the first model, different doses of the PSMA-Vδ2-Fc bsTCE were injected alone or in combination with the reference IgG1 antibody trastuzumab into Tg32 severe combined immunodeficient (SCID) transgenic mice that expressed the human FcRn (Figure 7C). Quantification of the amount of antibody in blood samples collected at different timepoints indicated that the PSMA-Vδ2-Fc bsTCE had a half-life that ranged between 5.83 ± 0.42 days (2 mg/kg), 6.67 ± 0.42 days (5 mg/kg), and 7.15 ± 0.44 days (10 mg/kg). Addition of trastuzumab did not impact the half-life since the half-life of 5 mg/mL PSMA-Vδ2-Fc bsTCE without trastuzumab injection was not significantly different (6.99 ± 0.10 days). The half-life of trastuzumab was comparable in all groups and similar to the half-life of the PSMA-Vδ2Fc bsTCE ranging between 5.11 ± 0.44 days (2 mg/mL), 4.71 ± 0.11 days (5 mg/mL), and 5.76 ± 0.33 days (10 mg/mL). More details regarding kinetic parameters can be found in Table S3. A second pharmacokinetic assessment of the PSMA-Vδ2-Fc bsTCE was done in female cynomolgus monkeys (*Macaca fascicularis*) because of the high homology between their FcRn and human FcRn. Plasma samples were collected at different timepoints after a single intravenous administration of 0.03, 1.0, or 3.0 mg/kg PSMA-Vδ2-Fc bsTCE doses. As Figure 7D illustrates, the plasma half-life of the PSMA-Vδ2-Fc bsTCE ranged between 6.75 days (0.03 mg/kg), 6.25 days (1.0 mg/kg), and 6.91 days (3.0 mg/kg) and was thus comparable to that observed in the murine Tg32 SCID transgenic model. More details regarding kinetic parameters can be found in Table S4. Thus, the PSMA-Vδ2-Fc bsTCE shows favorable pharmacokinetic properties in line with the IgG1 antibody trastuzumab.

## PSMA-Vδ2-Fc bsTCE reactivity follows the expected expression patterns of PSMA and Vγ9Vδ2-TCR in healthy human tissues

In order to assess the human tissue reactivity of the PSMA-Vδ2-Fc bsTCE, the molecule was FITC-labeled to be able to detect it using a secondary anti-FITC detection method in IHC. We first established that the labeling of the bsTCE did not affect binding affinity to either Vγ9Vδ2 T cells (Vγ9Vδ2 T cell binding $EC_{50}$ = 1.41 nM (FITC-labeled PSMA-Vδ2-Fc bsTCE) versus 0.97 nM (PSMA-Vδ2-Fc bsTCE)) or PSMA-expressing LNCaP cells (LNCaP binding $EC_{50}$ 6.00 nM (FITC-labeled PSMA-Vδ2-Fc bsTCE) versus 6.28 nM (PSMA-Vδ2-Fc bsTCE)) (Figure 8A; Vγ9Vδ2 T cells, binding assessed by flow cytometry and 8B; LNCaP cells, binding assessed by ELISA). Reactivity to a panel of 42 different frozen normal human tissues and blood smears (three donors per tissue/blood smear) was subsequently tested and showed moderate to marked membrane staining (with some variable cytoplasmic staining) in acinar cells of the prostate; low intensity, mainly cytoplasmic, staining in acinar cells of the parotid gland in three out of three donors, and minimal

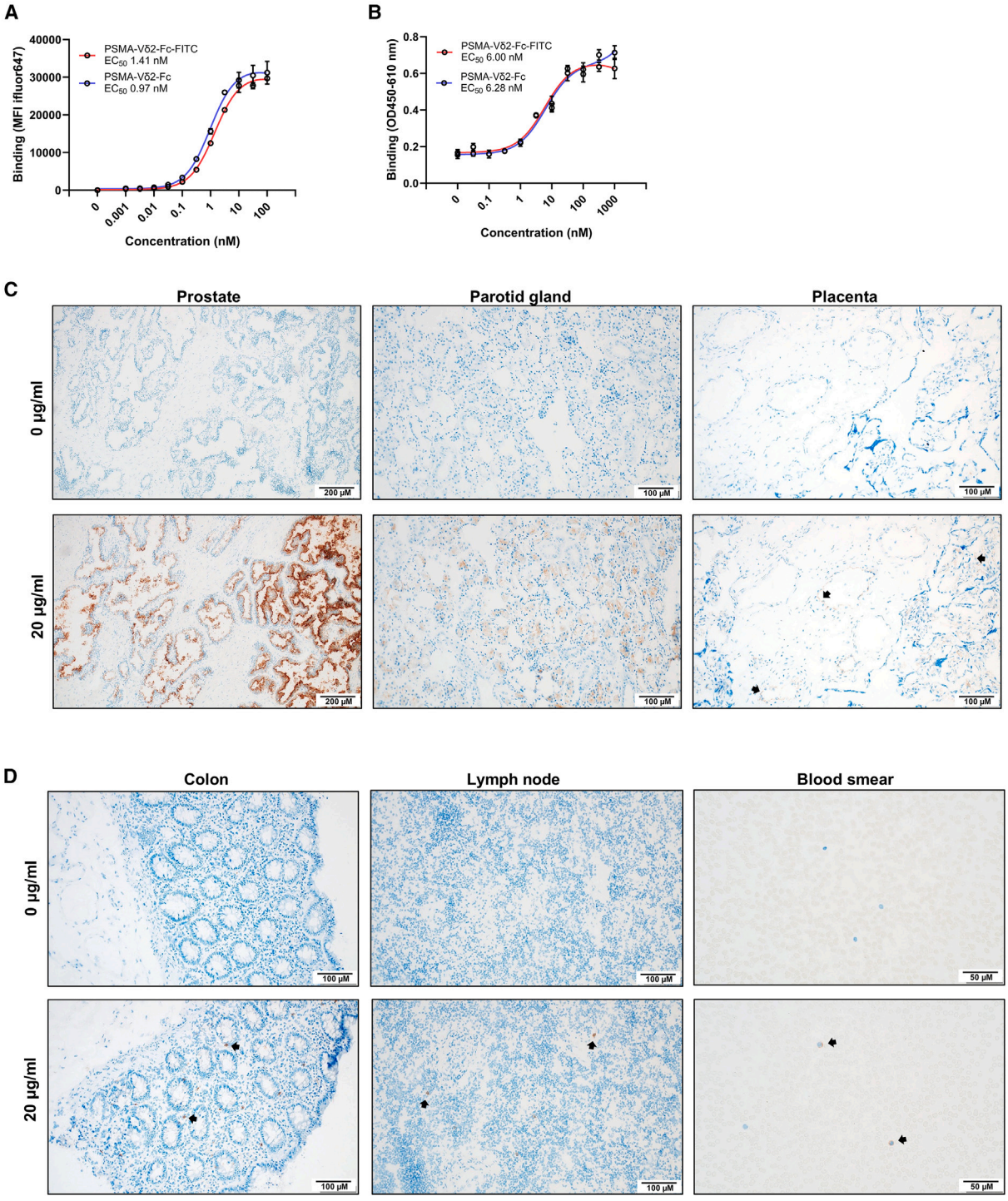


**Figure 8. Binding analysis of PSMA-Vδ2-Fc bsTCE using immunohistochemistry**

(A and B) FITC-labeled PSMA-Vδ2-Fc bsTCE and/or PSMA-Vδ2-Fc bsTCE binding to (A) Vγ9Vδ2 T cell lines ($n$ = 2) and (B) LNCaP tumor cells ($n$ = 2).
(C and D) Representative images of binding of 0 or 20 μg/mL FITC-labeled PSMA-Vδ2-Fc bsTCE to a panel of frozen normal human tissues and a blood smear from donors. Binding was detected with a secondary goat anti-FITC antibody (brown) combined with hematoxylin and bluing reagent to stain cell nuclei (blue). Data were generated using flow cytometry (A) and ELISA (B) and represent mean ± S.E.M. or IHC (C and D). Black arrows indicate staining-positive Vδ2$^+$ T cells. As specified in each subfigure, scale bars indicate 50, 100 or 200 μm.

staining in fusiform cells of blood vessels and placenta villi (considered to represent endothelial cells) in the placenta of one out of three donors (representative images are shown in Figure 8C). No reactivity was detected in a wide range of other tissue samples (adrenal, blood smears, breast, small and large intestines, gall bladder, kidney, liver, lung, lymph node, nerve, ovary, oviduct, spleen, testis, thymus, tonsil, ureter, urinary bladder, cervix, and uterus endometrium) with the exception of incidental reactivity to membranes of lymphocyte-like cells, which were most likely Vγ9Vδ2 T cells binding to the Vδ2-VHH (representative images are shown in Figure 8D). This tissue reactivity analysis of the PSMA-Vδ2-Fc bsTCE therefore was in line with the known tissue expression of PSMA (i.e., prostate, parotid glands, and placenta[25,33]) and Vγ9Vδ2 T cells and did not reveal unexpected off-target reactivity.

## DISCUSSION

Patients with metastatic PCa are initially treated with androgen-deprivation therapy but tumors typically progress over time to castration-resistant PCa which remains an incurable and fatal disease.[5,6] Although immunotherapeutic approaches have offered tremendous progress in the treatment of many cancer indications, in PCa these have failed to achieve a significant benefit for the great majority of patients. This lack of success is likely due to the immunosuppressive tumor microenvironment in PCa and the general lack of infiltration by effector T cells.[10–13] Vγ9Vδ2 T cells however have been reported to be present in tumors labeled as immunologically "cold" and their high-cytotoxic capacity and ability to activate other immune cells may offer the opportunity to transform the microenvironment in such tumors to a more immune permissive state.[14,17,18] Therapies stimulating Vγ9Vδ2 T cells in cancer patients through the use of nitrogen-containing aminobisphosphonates (nBP) like pamidronate or zoledronic acid, in combination with low dose IL-2 or adoptive transfer of Vγ9Vδ2 T cells are well tolerated and safe. While some partial or complete remissions have been observed, these approaches overall failed to provide consistent clinical benefit.[34–36] Here, we set out to explore the possibility to move from systemic activation of Vγ9Vδ2 T cells to a tumor-targeted approach by generating bispecific antibodies that can redirect Vγ9Vδ2 T cell reactivity to PSMA, which is overexpressed in primary and metastatic PCa tissues compared to non-malignant prostate tissue.[25,26] PSMA-Vδ2 bsTCE were initially tested using expanded healthy donor-derived Vγ9Vδ2 T cells and various PSMA expressing tumor cell lines, demonstrating potent Vγ9Vδ2 T cell activation and effector cytokine release as well as killing of PSMA-expressing tumor cells. These features were maintained when bsTCE were optimized for future clinical use (i.e., humanized and half-life extended). Though infiltration of Vγ9Vδ2 T cells in PCa had previously been reported,[14,37] we confirmed the presence of these cells in both malignant and non-malignant portions of prostate tissue samples of patients undergoing radical prostatectomy and found that the frequency of Vγ9Vδ2 T cells in these tissues was in the same range as in PCa patient peripheral blood. The majority of Vγ9Vδ2 T cells in both peripheral blood and in prostate tissue were found to express CD69. While CD69 is associated with early activation as well as tissue residency, the observation that levels of the activation marker 4-1BB were generally low on Vγ9Vδ2 T cells in tissue may suggest that here CD69 expression is more reflective of the tissue resident nature of these cells. Expression of PD-1 and CD57 was common but more variable on Vγ9Vδ2 T cells from PCa patients and was more prominent on Vγ9Vδ2 T cells in malignant prostate tissue. On conventional T cells, PD-1 and CD57 have been considered markers of activation/exhaustion and senescence, respectively, and both possibly associated with chronic antigen stimulation.[38] Recent studies found that highly cytotoxic $CD4^+$ and $CD8^+$ T cells expressing both PD-1 and CD57 were associated with survival and are responsive to immune checkpoint blockade.[39–41] Whether this is similarly the case for PD-1 and CD57 expression on Vγ9Vδ2 T cells is yet to be determined. Of interest, CD57 has also been indicated as a marker for memory differentiation in Vγ9Vδ2 T cells[42] and PD-1 and CD57 co-expression has been speculated to be reflective of anti-tumor effector functions rather than a sign of an impaired immune response.[43] In line with this notion, our analyses using prostate tumor tissue-derived and blood-derived Vγ9Vδ2 T cells confirmed PCa patient Vγ9Vδ2 T cell reactivity and effector functions in response to the PSMA-Vδ2 bsTCE. A similar preservation of effector functions was also reported for $PD\text{-}1^+TIM\text{-}3^+$ $V\delta2^+$ T cells in acute myeloid leukemia (AML) patients after treatment with anti-PD-1 and anti-TIM-3 blocking antibodies.[44]

Importantly, when exposed to PSMA-Vδ2 bsTCEs, Vγ9Vδ2 T cells were found to trigger lysis of prostate tumor cells with limited effects on normal prostate cells. This tumor specific activity may be related to differences in expression of PSMA as well as other receptors known to be involved in Vγ9Vδ2 T cell reactivity. Indeed, compared to non-malignant prostate cells, malignant prostate cells expressed higher levels of PSMA as well as higher levels of BTN3A and BTN2A1 (both critical for pAg sensing of Vγ9Vδ2 T cells), and more of the DNAM-1 ligands nectin-2 and PVR, as well as NKG2D ligands MIC-A/B, ULBP-3. and ULBP-2/5/6. In the absence of bsTCE or in the presence of sub-optimal concentrations of the PSMA-Vδ2-Fc bsTCE, DNAM-1, and NKG2D interactions were found to contribute to the tumor reactivity of Vγ9Vδ2 T cells. As BTN3A and NKG2D were found to contribute to Vγ9Vδ2 T cell reactivity in our earlier work using a CD1d-Vδ2[45] and an epidermal growth factor receptor (EGFR)-Vδ2 bsTCE[46] respectively, it is likely that the impact of co-receptors on tumor reactivity of Vγ9Vδ2 T cells may differ depending on the make-up of the respective receptor profiles on both the tumor and Vγ9Vδ2 T cell population. At functionally saturating concentrations of the PSMA-Vδ2-Fc bsTCE an impact of these co-receptors could not be detected.

The anti-tumor potential of PSMA-Vδ2 bsTCE was confirmed in a xenograft mouse model using PBMC as effector cells. Of note, although the Vγ9Vδ2 T cell frequency in these PBMC donors was relatively high, the Vγ9Vδ2 T cells in these PBMCs were neither enriched nor pre-activated *ex vivo*. Yet, their activation via the bsTCE in the *in vivo* model resulted in >60% tumor growth inhibition despite the low (initial) Vγ9Vδ2 T cell to tumor cell ratios of 1:22 and 1:60. It is possible that other immune cell subsets may have contributed to the observed tumor kill. Previously, we have shown activation of conventional T cells and NK

cells via IFN-γ and TNF production by Vγ9Vδ2 T cells activated using an EGFR-Vδ2 bsTCE.[46] In the current study, we additionally showed that bsTCEs can enhance the ability of Vγ9Vδ2 T cells to act as APCs to activate (tumor) antigen specific $CD8^+$ T cells. This interplay with other immune cells could possibly tip the balance toward a more inflamed tumor microenvironment containing (re-)activated effector cells, which might be further function-enhanced in combination with other immune-activating approaches, such as PD-1 immune checkpoint inhibition.

In recent years, PSMA has proven to be a relevant therapeutic target in metastatic castration-resistant prostate cancer (mCRPC) with the approval of lutetium-177-PSMA-617 radio-ligand therapy[7] and several other PSMA-targeted agents in development, including PSMA directed radioligands,[47] antibody-drug conjugates,[48] chimeric antigen receptor (CAR) T cells,[49] and bispecific CD3 T cell engagers.[49] Of note, while the median 4 months increase in overall survival of mCRPC patients treated with lutetium-177-PSMA-617 radioligand therapy is meaningful,[7] there is a strong need for more efficacious therapeutics that ideally also avoid some of the on-target off-tumor toxicity associated with the approved PSMA directed therapy, which include oral toxicities such as dry mouth.[50] Other challenges currently noted in the development of in particular CAR T cell and bispecific pan T cell engager therapies also need to be addressed: e.g., high-grade cytokine release syndrome, neurotoxicity, as well as immune-related deaths with PSMA-directed bispecific T cell engagers.[51–54] The data in this paper as well as our earlier work indicate that the intrinsic ability of Vγ9Vδ2 T cells to selectively interact with tumor cells is fairly well maintained in the presence of Vδ2 bsTCEs.[45,46,55] Vδ2 bsTCE are also expected to reduce the risk of high-grade CRS. Indeed, in multiple non-human primates (NHP) studies designed to explore toxicity with cross-reactive surrogate γδ T cell engagers directed against CD1d or EGFR, no relevant signs of toxicity were observed.[46,55] Finally, and in contrast to pan (CD3-based) T cell engagers,[56–58] Vδ2 bsTCEs do not cause detrimental co-activation of suppressive regulatory T cells, which are present in increased frequencies in PCa patients and that are associated with poor outcome.[59,60] Therefore, the PSMA-Vδ2 bsTCE described here is expected to result in a better overall therapeutic window.

To conclude, we here describe the development of a humanized half-life extended PSMA-Vδ2-Fc bsTCE that contains mutations known to silence Fc-mediated effector functions, shows no off-target binding in tissue cross-reactivity studies, and effectively induced antitumor immune responses against PCa in *in vitro*, *ex vivo*, and *in vivo* models with the potential for a broader antitumor immune response via increased bsTCE-triggered Vγ9Vδ2 T cell APC activity. The results reported here have formed the basis for the initiation of a phase 1/2a clinical trial in patients with therapy refractory metastatic castration-resistant prostate cancer (NCT05369000).

### Limitations of the study

The findings of this study are based on data collected from *in vitro*, *ex vivo*, and *in vivo* (animal) models. Clinical trials will be necessary to further validate these results.

The influence of sex on the results could not be determined because all prostate cancer patients in the study were male.

## RESOURCE AVAILABILITY

### Lead contact

Further information and requests for resources and reagents should be directed to and will be fulfilled by the lead contact, Lisa A. King (l.king@amsterdamumc.nl).

### Materials availability

There are restrictions to the availability of the generated PSMA-Vδ2 bsTCEs which are covered by intellectual property rights (publication number: 20230272110).

### Data and code availability

- All data reported in this paper can be shared by the lead contact upon reasonable request.
- This paper does not report original code.
- Any additional information required to reanalyze the data reported in this paper is available from the lead contact upon request.

## ACKNOWLEDGMENTS

We thank all the PCa patients who agreed to donate samples for this study. This research was funded by Lava Therapeutics N.V..

## AUTHOR CONTRIBUTIONS

L.A.K., H.J.v.d.V., and T.D.d.G. contributed to conception and design of the study; L.A.K., M.V., V.I.-G., I.B., and J.K. performed the experiments; L.A.K., V.I.-G., and I.B. performed experimental analysis and interpreted the results; H.J.v.d.V. and T.D.d.G. provided supervision; L.A.K. wrote the first draft of the manuscript; V.I.-G., A.N.V., R.C.R., D.L.H., T.R., A.E.P.A., P.W.H.I.P., P.M.v.H., T.D.d.G., and H.J.v.d.V. reviewed and revised the manuscript.

## DECLARATION OF INTERESTS

L.A.K., M.V.,and J.K. are/were funded by Lava Therapeutics NV. T.R., R.C.R., A.E.P.A., P.W.H.I.P., T.D.d.G.,and H.J.v.d.V. own Lava Therapeutics NV shares. V.I.-G., I.B., R.C.R., D.L.H., T.R., A.E.P.A., P.W.H.I.P., and H.J.v.d.V. are/were employees of Lava Therapeutics NV. T.D.d.G.is scientific advisor to Lava Therapeutics NV. Patent registration related to this work: Antibodies that bind PSMA and gamma-delta T cell receptors, Lava Therapeutics NV, WO2022008646A1, 2022-01-13.

## STAR★METHODS

Detailed methods are provided in the online version of this paper and include the following:

- KEY RESOURCES TABLE
- EXPERIMENTAL MODEL AND STUDY PARTICIPANT DETAILS
  - Design, production, purification and humanization of bsTCEs
  - Tumor cell lines
  - Generation of LNCaP PSMA knock-out cell line
  - PBMC isolation and T cell cultures
  - PCa patient tissue samples
  - *In vivo* tumor rejection
  - *In vivo* pharmacokinetics of the PSMA-Vδ2-Fc bsTCE
- METHOD DETAILS
  - Flow cytometry
  - Assessment of target specificity and binding characteristics of bsTCEs
  - Assessment of Vγ9Vδ2 T cell activation
  - Assessment of target cell lysis
  - Assessment of APC function of Vγ9Vδ2 T cells
  - Tissue-cross reactivity
- QUANTIFICATION AND STATISTICAL ANALYSIS

## SUPPLEMENTAL INFORMATION

Supplemental information can be found online at https://doi.org/10.1016/j.isci.2024.111289.

Received: May 9, 2024
Revised: August 17, 2024
Accepted: October 28, 2024
Published: October 30, 2024

## REFERENCES

1. Sung, H., Ferlay, J., Siegel, R.L., Laversanne, M., Soerjomataram, I., Jemal, A., and Bray, F. (2021). Global Cancer Statistics 2020: GLOBOCAN Estimates of Incidence and Mortality Worldwide for 36 Cancers in 185 Countries. CA A Cancer J. Clin. *71*, 209–249. https://doi.org/10.3322/caac.21660.
2. Aragon-Ching, J.B., Williams, K.M., and Gulley, J.L. (2007). Impact of androgen-deprivation therapy on the immune system: implications for combination therapy of prostate cancer. Front. Biosci. *12*, 4957–4971. https://doi.org/10.2741/2441.
3. Drake, C.G. (2010). Prostate cancer as a model for tumour immunotherapy. Nat. Rev. Immunol. *10*, 580–593. https://doi.org/10.1038/nri2817.
4. Klotz, L., O'Callaghan, C., Ding, K., Toren, P., Dearnaley, D., Higano, C.S., Horwitz, E., Malone, S., Goldenberg, L., Gospodarowicz, M., and Crook, J.M. (2015). Nadir testosterone within first year of androgen-deprivation therapy (ADT) predicts for time to castration-resistant progression: a secondary analysis of the PR-7 trial of intermittent versus continuous ADT. J. Clin. Oncol. *33*, 1151–1156. https://doi.org/10.1200/JCO.2014.58.2973.
5. Posdzich, P., Darr, C., Hilser, T., Wahl, M., Herrmann, K., Hadaschik, B., and Grünwald, V. (2023). Metastatic Prostate Cancer-A Review of Current Treatment Options and Promising New Approaches. Cancers *15*, 461. https://doi.org/10.3390/cancers15020461.
6. Muniyan, S., Li, B., and Batra, S.K. (2022). Editorial: Metastatic Castration Resistant Prostate Cancer: Prognosis and Treatment. Front. Oncol. *12*, 913630. https://doi.org/10.3389/fonc.2022.913630.
7. Sartor, O., de Bono, J., Chi, K.N., Fizazi, K., Herrmann, K., Rahbar, K., Tagawa, S.T., Nordquist, L.T., Vaishampayan, N., El-Haddad, G., et al. (2021). Lutetium-177-PSMA-617 for Metastatic Castration-Resistant Prostate Cancer. N. Engl. J. Med. *385*, 1091–1103. https://doi.org/10.1056/NEJMoa2107322.
8. Cai, M., Song, X.L., Li, X.A., Chen, M., Guo, J., Yang, D.H., Chen, Z., and Zhao, S.C. (2023). Current therapy and drug resistance in metastatic castration-resistant prostate cancer. Drug Resist. Updates *68*, 100962. https://doi.org/10.1016/j.drup.2023.100962.
9. Marcus, L., Lemery, S.J., Keegan, P., and Pazdur, R. (2019). FDA Approval Summary: Pembrolizumab for the Treatment of Microsatellite Instability-High Solid Tumors. Clin. Cancer Res. *25*, 3753–3758. https://doi.org/10.1158/1078-0432.CCR-18-4070.
10. Fay, E.K., and Graff, J.N. (2020). Immunotherapy in Prostate Cancer. Cancers *12*, 1752. https://doi.org/10.3390/cancers12071752.
11. Sfanos, K.S., Bruno, T.C., Maris, C.H., Xu, L., Thoburn, C.J., DeMarzo, A.M., Meeker, A.K., Isaacs, W.B., and Drake, C.G. (2008). Phenotypic analysis of prostate-infiltrating lymphocytes reveals TH17 and Treg skewing. Clin. Cancer Res. *14*, 3254–3261. https://doi.org/10.1158/1078-0432.CCR-07-5164.
12. Bilusic, M., Madan, R.A., and Gulley, J.L. (2017). Immunotherapy of Prostate Cancer: Facts and Hopes. Clin. Cancer Res. *23*, 6764–6770. https://doi.org/10.1158/1078-0432.CCR-17-0019.
13. Hirz, T., Mei, S., Sarkar, H., Kfoury, Y., Wu, S., Verhoeven, B.M., Subtelny, A.O., Zlatev, D.V., Wszolek, M.W., Salari, K., et al. (2023). Dissecting the immune suppressive human prostate tumor microenvironment via integrated single-cell and spatial transcriptomic analyses. Nat. Commun. *14*, 663. https://doi.org/10.1038/s41467-023-36325-2.
14. Tosolini, M., Pont, F., Poupot, M., Vergez, F., Nicolau-Travers, M.L., Vermijlen, D., Sarry, J.E., Dieli, F., and Fournié, J.J. (2017). Assessment of tumor-infiltrating TCRVgamma9Vdelta2 gammadelta lymphocyte abundance by deconvolution of human cancers microarrays. OncoImmunology *6*, e1284723. https://doi.org/10.1080/2162402X.2017.1284723.
15. Harly, C., Guillaume, Y., Nedellec, S., Peigné, C.M., Mönkkönen, H., Mönkkönen, J., Li, J., Kuball, J., Adams, E.J., Netzer, S., et al. (2012). Key implication of CD277/butyrophilin-3 (BTN3A) in cellular stress sensing by a major human gammadelta T-cell subset. Blood *120*, 2269–2279. https://doi.org/10.1182/blood-2012-05-430470.
16. Rigau, M., Ostrouska, S., Fulford, T.S., Johnson, D.N., Woods, K., Ruan, Z., McWilliam, H.E.G., Hudson, C., Tutuka, C., Wheatley, A.K., et al. (2020). Butyrophilin 2A1 is essential for phosphoantigen reactivity by gammadelta T cells. Science *367*, eaay5516. https://doi.org/10.1126/science.aay5516.
17. Chien, Y.-h., Meyer, C., and Bonneville, M. (2014). γδ T Cells: First Line of Defense and Beyond. Annu. Rev. Immunol. *32*, 121–155. https://doi.org/10.1146/annurev-immunol-032713-120216.
18. Hayday, A.C. (2019). gammadelta T Cell Update: Adaptate Orchestrators of Immune Surveillance. J. Immunol. *203*, 311–320. https://doi.org/10.4049/jimmunol.1800934.
19. Kunzmann, V., Bauer, E., Feurle, J., Weissinger, F., Tony, H.P., and Wilhelm, M. (2000). Stimulation of gammadelta T cells by aminobisphosphonates and induction of antiplasma cell activity in multiple myeloma. Blood *96*, 384–392.
20. Todaro, M., D'Asaro, M., Caccamo, N., Iovino, F., Francipane, M.G., Meraviglia, S., Orlando, V., La Mendola, C., Gulotta, G., Salerno, A., et al. (2009). Efficient killing of human colon cancer stem cells by gammadelta T lymphocytes. J. Immunol. *182*, 7287–7296. https://doi.org/10.4049/jimmunol.0804288.
21. D'Asaro, M., La Mendola, C., Di Liberto, D., Orlando, V., Todaro, M., Spina, M., Guggino, G., Meraviglia, S., Caccamo, N., Messina, A., et al. (2010). V gamma 9V delta 2 T lymphocytes efficiently recognize and kill zoledronate-sensitized, imatinib-sensitive, and imatinib-resistant chronic myelogenous leukemia cells. J. Immunol. *184*, 3260–3268. https://doi.org/10.4049/jimmunol.0903454.
22. Mattarollo, S.R., Kenna, T., Nieda, M., and Nicol, A.J. (2007). Chemotherapy and zoledronate sensitize solid tumour cells to Vgamma9Vdelta2 T cell cytotoxicity. Cancer Immunol. Immunother. *56*, 1285–1297. https://doi.org/10.1007/s00262-007-0279-2.
23. Sawaisorn, P., Tangchaikeeree, T., Chan-On, W., Leepiyasakulchai, C., Udomsangpetch, R., Hongeng, S., and Jangpatarapongsa, K. (2019). Antigen-Presenting Cell Characteristics of Human gammadelta T Lymphocytes in Chronic Myeloid Leukemia. Immunol. Invest. *48*, 11–26. https://doi.org/10.1080/08820139.2018.1529039.
24. Holmen Olofsson, G., Idorn, M., Carnaz Simões, A.M., Aehnlich, P., Skadborg, S.K., Noessner, E., Debets, R., Moser, B., Met, Ö., and Thor Straten, P. (2021). Vγ9Vδ2 T Cells Concurrently Kill Cancer Cells and Cross-Present Tumor Antigens. Front. Immunol. *12*, 645131. https://doi.org/10.3389/fimmu.2021.645131.
25. Silver, D.A., Pellicer, I., Fair, W.R., Heston, W.D., and Cordon-Cardo, C. (1997). Prostate-specific membrane antigen expression in normal and malignant human tissues. Clin. Cancer Res. *3*, 81–85.
26. Troyer, J.K., Beckett, M.L., and Wright, G.L., Jr. (1995). Detection and characterization of the prostate-specific membrane antigen (PSMA) in tissue extracts and body fluids. Int. J. Cancer *62*, 552–558. https://doi.org/10.1002/ijc.2910620511.
27. Chatalic, K.L.S., Veldhoven-Zweistra, J., Bolkestein, M., Hoeben, S., Koning, G.A., Boerman, O.C., de Jong, M., and van Weerden, W.M. (2015). A Novel (1)(1)(1)In-Labeled Anti-Prostate-Specific Membrane Antigen Nanobody for Targeted SPECT/CT Imaging of Prostate Cancer. J. Nucl. Med. *56*, 1094–1099. https://doi.org/10.2967/jnumed.115.156729.

28. de Bruin, R.C.G., Lougheed, S.M., van der Kruk, L., Stam, A.G., Hooijberg, E., Roovers, R.C., van Bergen En Henegouwen, P.M.P., Verheul, H.M.W., de Gruijl, T.D., and van der Vliet, H.J. (2016). Highly specific and potently activating Vgamma9Vdelta2-T cell specific nanobodies for diagnostic and therapeutic applications. Clin. Immunol. *169*, 128–138. https://doi.org/10.1016/j.clim.2016.06.012.

29. Brandes, M., Willimann, K., and Moser, B. (2005). Professional antigen-presentation function by human gammadelta T Cells. Science *309*, 264–268. https://doi.org/10.1126/science.1110267.

30. Brandes, M., Willimann, K., Bioley, G., Lévy, N., Eberl, M., Luo, M., Tampé, R., Lévy, F., Romero, P., and Moser, B. (2009). Cross-presenting human gammadelta T cells induce robust CD8+ alphabeta T cell responses. Proc Natl Acad Sci USA *106*, 2307–2312. https://doi.org/10.1073/pnas.0810059106.

31. Meuter, S., Eberl, M., and Moser, B. (2010). Prolonged antigen survival and cytosolic export in cross-presenting human gammadelta T cells. Proc. Natl. Acad. Sci. USA *107*, 8730–8735. https://doi.org/10.1073/pnas.1002769107.

32. Jin, P., Han, T.H., Ren, J., Saunders, S., Wang, E., Marincola, F.M., and Stroncek, D.F. (2010). Molecular signatures of maturing dendritic cells: implications for testing the quality of dendritic cell therapies. J. Transl. Med. *8*, 4. https://doi.org/10.1186/1479-5876-8-4.

33. Heynickx, N., Herrmann, K., Vermeulen, K., Baatout, S., and Aerts, A. (2021). The salivary glands as a dose limiting organ of PSMA- targeted radionuclide therapy: A review of the lessons learnt so far. Nucl. Med. Biol. *98–99*, 30–39. https://doi.org/10.1016/j.nucmedbio.2021.04.003.

34. Pressey, J.G., Adams, J., Harkins, L., Kelly, D., You, Z., and Lamb, L.S., Jr. (2016). In vivo expansion and activation of gammadelta T cells as immunotherapy for refractory neuroblastoma: A phase 1 study. Medicine (Baltim.) *95*, e4909. https://doi.org/10.1097/MD.0000000000004909.

35. Dieli, F., Vermijlen, D., Fulfaro, F., Caccamo, N., Meraviglia, S., Cicero, G., Roberts, A., Buccheri, S., D'Asaro, M., Gebbia, N., et al. (2007). Targeting human gammadelta T cells with zoledronate and interleukin-2 for immunotherapy of hormone-refractory prostate cancer. Cancer Res. *67*, 7450–7457. https://doi.org/10.1158/0008-5472.CAN-07-0199.

36. Giannotta, C., Autino, F., and Massaia, M. (2023). Vgamma9Vdelta2 T-cell immunotherapy in blood cancers: ready for prime time? Front. Immunol. *14*, 1167443. https://doi.org/10.3389/fimmu.2023.1167443.

37. Vella, M., Coniglio, D., Abrate, A., Scalici Gesolfo, C., Lo Presti, E., Meraviglia, S., Serretta, V., and Simonato, A. (2019). Characterization of human infiltrating and circulating gamma-delta T cells in prostate cancer. Investig. Clin. Urol. *60*, 91–98. https://doi.org/10.4111/icu.2019.60.2.91.

38. Muroyama, Y., and Wherry, E.J. (2021). Memory T-Cell Heterogeneity and Terminology. Cold Spring Harbor Perspect. Biol. *13*, a037929. https://doi.org/10.1101/cshperspect.a037929.

39. Jubel, J.M., Barbati, Z.R., Burger, C., Wirtz, D.C., and Schildberg, F.A. (2020). The Role of PD-1 in Acute and Chronic Infection. Front. Immunol. *11*, 487. https://doi.org/10.3389/fimmu.2020.00487.

40. Fehlings, M., Kim, L., Guan, X., Yuen, K., Tafazzol, A., Sanjabi, S., Zill, O.A., Rishipathak, D., Wallace, A., Nardin, A., et al. (2022). Single-cell analysis reveals clonally expanded tumor-associated CD57(+) CD8 T cells are enriched in the periphery of patients with metastatic urothelial cancer responding to PD-L1 blockade. J. Immunother. Cancer *10*, e004759. https://doi.org/10.1136/jitc-2022-004759.

41. Ramello, M.C., Núñez, N.G., Tosello Boari, J., Bossio, S.N., Canale, F.P., Abrate, C., Ponce, N., Del Castillo, A., Ledesma, M., Viel, S., et al. (2021). Polyfunctional KLRG-1(+)CD57(+) Senescent CD4(+) T Cells Infiltrate Tumors and Are Expanded in Peripheral Blood From Breast Cancer Patients. Front. Immunol. *12*, 713132. https://doi.org/10.3389/fimmu.2021.713132.

42. Rancan, C., Arias-Badia, M., Dogra, P., Chen, B., Aran, D., Yang, H., Luong, D., Ilano, A., Li, J., Chang, H., et al. (2023). Exhausted intratumoral Vdelta2(-) gammadelta T cells in human kidney cancer retain effector function. Nat. Immunol. *24*, 612–624. https://doi.org/10.1038/s41590-023-01448-7.

43. Pauza, C.D., Liou, M.L., Lahusen, T., Xiao, L., Lapidus, R.G., Cairo, C., and Li, H. (2018). Gamma Delta T Cell Therapy for Cancer: It Is Good to be Local. Front. Immunol. *9*, 1305. https://doi.org/10.3389/fimmu.2018.01305.

44. Wu, K., Feng, J., Xiu, Y., Li, Z., Lin, Z., Zhao, H., Zeng, H., Xia, W., Yu, L., and Xu, B. (2020). Vdelta2 T cell subsets, defined by PD-1 and TIM-3 expression, present varied cytokine responses in acute myeloid leukemia patients. Int. Immunopharm. *80*, 106122. https://doi.org/10.1016/j.intimp.2019.106122.

45. de Weerdt, I., Lameris, R., Ruben, J.M., de Boer, R., Kloosterman, J., King, L.A., Levin, M.D., Parren, P.W.H.I., de Gruijl, T.D., Kater, A.P., and van der Vliet, H.J. (2021). A Bispecific Single-Domain Antibody Boosts Autologous Vgamma9Vdelta2-T Cell Responses Toward CD1d in Chronic Lymphocytic Leukemia. Clin. Cancer Res. *27*, 1744–1755. https://doi.org/10.1158/1078-0432.CCR-20-4576.

46. King, L.A., Toffoli, E.C., Veth, M., Iglesias-Guimarais, V., Slot, M.C., Amsen, D., van de Ven, R., Derks, S., Fransen, M.F., Tuynman, J.B., et al. (2023). A bispecific gammadelta T-cell engager targeting EGFR activates a potent Vgamma9Vdelta2 T cell-mediated immune response against EGFR-expressing tumors. Cancer Immunol. Res. *11*, 1237–1252. https://doi.org/10.1158/2326-6066.CIR-23-0189.

47. Jang, A., Kendi, A.T., and Sartor, O. (2023). Status of PSMA-targeted radioligand therapy in prostate cancer: current data and future trials. Ther. Adv. Med. Oncol. *15*, 17588359231157632. https://doi.org/10.1177/17588359231157632.

48. Sardinha, M., Palma Dos Reis, A.F., Barreira, J.V., Fontes Sousa, M., Pacey, S., and Luz, R. (2023). Antibody-Drug Conjugates in Prostate Cancer: A Systematic Review. Cureus *15*, e34490. https://doi.org/10.7759/cureus.34490.

49. Zarrabi, K.K., Narayan, V., Mille, P.J., Zibelman, M.R., Miron, B., Bashir, B., and Kelly, W.K. (2023). Bispecific PSMA antibodies and CAR-T in metastatic castration-resistant prostate cancer. Ther. Adv. Urol. *15*, 17562872231182219. https://doi.org/10.1177/17562872231182219.

50. Emperumal, C.P., Villa, A., Hwang, C., Oh, D., Fong, L., Aggarwal, R., and Keenan, B.P. (2024). Oral Toxicities of PSMA-Targeted Immunotherapies for The Management of Prostate Cancer. Clin. Genitourin. Cancer *22*, 380–384. https://doi.org/10.1016/j.clgc.2023.12.008.

51. Tran, B., Horvath, L., Dorff, T., Rettig, M., Lolkema, M., Machiels, J.P., Rottey, S., Autio, K., Greil, R., Adra, N., et al. (2020). 609O Results from a phase I study of AMG 160, a half-life extended (HLE), PSMA-targeted, bispecific T-cell engager (BiTE®) immune therapy for metastatic castration-resistant prostate cancer (mCRPC). Ann. Oncol. *31*, S507. https://doi.org/10.1016/j.annonc.2020.08.869.

52. Kamat, N.V., Yu, E.Y., and Lee, J.K. (2021). BiTE-ing into Prostate Cancer with Bispecific T-cell Engagers. Clin. Cancer Res. *27*, 2675–2677. https://doi.org/10.1158/1078-0432.CCR-21-0355.

53. De Bono, J.S., Fong, L., Beer, T.M., Gao, X., Geynisman, D.M., Burris III, H.A., Strauss, J.F., Courtney, K.D., Quinn, D.I., VanderWeele, D.J., et al. (2021). Results of an ongoing phase 1/2a dose escalation study of HPN424, a tri-specific half-life extended PSMA-targeting T-cell engager, in patients with metastatic castration-resistant prostate cancer (mCRPC). J. Clin. Oncol. *39*, 5013.

54. Zhang, J., Stein, M.N., Kelly, W.K., Tsao, C.K., Falchook, G.S., Xu, Y., Seebach, F.A., Lowy, I., Mohan, K.K., Kroog, G., and Miller, E. (2021). A phase I/II study of REGN5678 (Anti-PSMAxCD28, a costimulatory bispecific antibody) with cemiplimab (antiPD-1) in patients with metastatic castration-resistant prostate cancer. J. Clin. Oncol. *39*, 174.

55. Lameris, R., Ruben, J.M., Iglesias-Guimarais, V., de Jong, M., Veth, M., van de Bovenkamp, F.S., de Weerdt, I., Kater, A.P., Zweegman, S., Horbach, S., et al. (2023). A bispecific T cell engager recruits both type 1 NKT and Vgamma9Vdelta2-T cells for the treatment of CD1d-expressing hematological malignancies. Cell Rep. Med. *4*, 100961. https://doi.org/10.1016/j.xcrm.2023.100961.

56. Duell, J., Dittrich, M., Bedke, T., Mueller, T., Eisele, F., Rosenwald, A., Rasche, L., Hartmann, E., Dandekar, T., Einsele, H., and Topp, M.S. (2017). Frequency of regulatory T cells determines the outcome of the T-cell-engaging antibody blinatumomab in patients with B-precursor ALL. Leukemia *31*, 2181–2190. https://doi.org/10.1038/leu.2017.41.

57. Belmontes, B., Sawant, D.V., Zhong, W., Tan, H., Kaul, A., Aeffner, F., O'Brien, S.A., Chun, M., Noubade, R., Eng, J., et al. (2021). Immunotherapy combinations overcome resistance to bispecific T cell engager treatment in T cell-cold solid tumors. Sci. Transl. Med. *13*, eabd1524. https://doi.org/10.1126/scitranslmed.abd1524.

58. Middelburg, J., Kemper, K., Engelberts, P., Labrijn, A.F., Schuurman, J., and van Hall, T. (2021). Overcoming Challenges for CD3-Bispecific Antibody Therapy in Solid Tumors. Cancers *13*, 287. https://doi.org/10.3390/cancers13020287.

59. Idorn, M., Køllgaard, T., Kongsted, P., Sengeløv, L., and Thor Straten, P. (2014). Correlation between frequencies of blood monocytic myeloid-derived suppressor cells, regulatory T cells and negative prognostic markers in patients with castration-resistant metastatic prostate cancer. Cancer Immunol. Immunother. *63*, 1177–1187. https://doi.org/10.1007/s00262-014-1591-2.

60. Erlandsson, A., Carlsson, J., Lundholm, M., Fält, A., Andersson, S.O., Andrén, O., and Davidsson, S. (2019). M2 macrophages and regulatory T cells in lethal prostate cancer. Prostate *79*, 363–369. https://doi.org/10.1002/pros.23742.

61. McCoy, L.E., Quigley, A.F., Strokappe, N.M., Bulmer-Thomas, B., Seaman, M.S., Mortier, D., Rutten, L., Chander, N., Edwards, C.J., Ketteler, R., et al. (2012). Potent and broad neutralization of HIV-1 by a llama antibody elicited by immunization. J. Exp. Med. *209*, 1091–1103. https://doi.org/10.1084/jem.20112655.

62. Williams, D.G., Matthews, D.J., and Jones, T. (2010). Antibody Engineering Ch. Chapter 21, pp. 319–339.

63. Ye, J., Ma, N., Madden, T.L., and Ostell, J.M. (2013). IgBLAST: an immunoglobulin variable domain sequence analysis tool. Nucleic Acids Res. *41*, W34–W40. https://doi.org/10.1093/nar/gkt382.

64. Carter, P. (2001). Bispecific human IgG by design. J. Immunol. Methods *248*, 7–15. https://doi.org/10.1016/s0022-1759(00)00339-2.

65. Schütze, K., Petry, K., Hambach, J., Schuster, N., Fumey, W., Schriewer, L., Röckendorf, J., Menzel, S., Albrecht, B., Haag, F., et al. (2018). CD38-Specific Biparatopic Heavy Chain Antibodies Display Potent Complement-Dependent Cytotoxicity Against Multiple Myeloma Cells. Front. Immunol. *9*, 2553. https://doi.org/10.3389/fimmu.2018.02553.

66. Santegoets, S.J.A.M., Bontkes, H.J., Stam, A.G.M., Bhoelan, F., Ruizendaal, J.J., van den Eertwegh, A.J.M., Hooijberg, E., Scheper, R.J., and de Gruijl, T.D. (2008). Inducing antitumor T cell immunity: comparative functional analysis of interstitial versus Langerhans dendritic cells in a human cell line model. J. Immunol. *180*, 4540–4549. https://doi.org/10.4049/jimmunol.180.7.4540.

CellPress
OPEN ACCESS

## STAR★METHODS

### KEY RESOURCES TABLE

| REAGENT or RESOURCE | SOURCE | IDENTIFIER |
|---|---|---|
| Antibodies | | |
| PSMA-Vδ2 bsTCE | ImmunoPrecise antibodies | N/A (custom-made) |
| Vδ2-PSMA bsTCE | ImmunoPrecise antibodies | N/A (custom-made) |
| Humanized PSMA-Vδ2 bsTCE | ImmunoPrecise antibodies | N/A (custom-made) |
| Humanized PSMA-Vδ2-Fc bsTCE | ImmunoPrecise antibodies | N/A (custom-made) |
| gp120-gp120-Fc bsTCE | ImmunoPrecise antibodies | N/A (custom-made) |
| gp120-Vδ2-Fc bsTCE | ImmunoPrecise antibodies | N/A (custom-made) |
| PSMA-gp120-Fc bsTCE | ImmunoPrecise antibodies | N/A (custom-made) |
| DNAM-1 blocking antibody | BD Bioscience | Cat#559787; RRID: AB_397328 |
| NKG2D blocking antibody | R&D Systems | Cat#MAB139-100 |
| NKG2A blocking antibody | Proteogenics | Cat#PX-TA1392-100UG |
| BTN3A blocking antibody | Creative Biolabs | Cat#PABL-415; RRID: AB_3111655 |
| IgG1 isotype control | R&D Systems | Cat#MAB002; RRID: AB_357344 |
| HRP-conjugated goat α-FITC antibody | KPL | Cat#01-40-01 |
| rabbit anti-camelid VHH cocktail | GenScript | Cat#19L002038 |
| monoRab rabbit anti-camelid VHH-HRP conjugate | Genscript | Cat#A01861-200 |
| mouse anti-trastuzumab antibody | BioRad | Cat#HCA168 |
| HRP labeled-rabbit anti-camelid VHH-antibody | Genscript | Cat#A011861 |
| A*02:01-GILGFVFTL-dextramer | Immudex | Cat#WB2161-APC |
| A*02:01-NLVPMVATV-dextramer | Immudex | Cat#WB2132-APC |
| OKT3 | Thermo-Fisher Scientific | Cat#16-0037-81; RRID: AB_468854 |
| Chemicals, peptides, and recombinant proteins | | |
| ELAGIGILTV | ProImmune | N/A (custom-made) |
| LKTRPILSPLTKGILGFVFTLTVPSERGLQ | ProImmune | N/A (custom-made) |
| GHGHSYTTAEELAGIGILTVILGVL | ProImmune | N/A (custom-made) |
| TWPPWQAGILARNLVPMVATVQG QNLKYQE | ProImmune | N/A (custom-made) |
| NLVPMVATV | ProImmune | N/A (custom-made) |
| PSMA protein | Sino Biological | Cat#15877-H07H |
| IL-2 | Miltenyi Biotec | Cat#130-097-748 |
| IL-7 | R&D Systems | Cat#207-IL-025 |
| IL-15 | eBioscience | Cat#34-8159-85 |
| IL-15 | Miltenyi Biotec | Cat#130-095-766 |
| PHA | Thermo Fisher Scientific | Cat#R30852801 |
| Experimental models: Cell lines | | |
| LNCaP | American Type Culture Collection | Cat#CRL-1740 |
| PC3 | American Type Culture Collection | Cat#CRL-1435 |
| VCaP | European Collection of Authenticated Cell Cultures | Cat#06020201-1VL |
| 22Rv1 | European Collection of Authenticated Cell Cultures | Cat#5092802 |
| THP-1 | European Collection of Authenticated Cell Cultures | Cat#88081201 |

(*Continued on next page*)

*Continued*

| REAGENT or RESOURCE | SOURCE | IDENTIFIER |
|---|---|---|
| JY | European Collection of Authenticated Cell Cultures | Cat#94022533 |
| **Experimental models: Organisms/strains** | | |
| Mouse: NOD/ShiLtJGpt-Prkdcem26Cd52Il2rgem26Cd22/Gpt strain | Crown Bioscience (Taichang, China) | N/A |
| Mouse: B6.Cg-Fcgrt$^{tm1Dcr}$ Prkdc$^{scid}$ Tg [FCGRT]32DcrJ strain | The Jackson Laboratory (Bar Harbor, USA) | N/A |
| Non-human primates: *Macaca fascicularis* | Covance Laboratories Limited (Cambridgeshire, UK) | N/A |
| **Software and algorithms** | | |
| Kaluza Analysis Version 1.3 | Beckman Coulter | N/A |
| FlowJo Version 10.6.1 and 10.7.2 | Becton Dickinson | N/A |
| FCAP Array software v3.0 | BD | N/A |
| SoftMax Pro software v7.1 | Molecular Devices | N/A |
| GraphPad Prism v9.1.0 | GraphPad | N/A |
| **Other** | | |
| Anti-mouse IgG microbeads | Miltenyi Biotec | Cat#130-048-401 |
| EasySep$^{TM}$ human gamma/delta T cell negative isolation kit | STEMCELL Technologies | Cat#19255 |
| EasySep human CD8$^{+}$ T cell isolation kit | STEMCELL Technologies | Cat#17953 |
| CTS$^{TM}$ AIM-V$^{TM}$ Medium | Thermo-Fisher Scientific | Cat#A3830801 |
| RPMI medium | Gibco | Cat#22400089 |
| Fetal calf serum | Biological Industries | Cat#04-007-1A |
| β-mercaptoethanol | Biological Industries | Cat#200-646-6 |
| β-mercaptoethanol | Merck | Cat#M6250 |
| PSG | Life Technologies | Cat#10378-016 |
| RPMI 1640 ATCC modified medium | Thermo-Fisher Scientific | Cat#A10491-01 |
| Fetal bovine serum | Cytiva | Cat#SV30160.03 |
| Gentamycin | Gibco | Cat#15710-049 |
| RPMI 1640 medium | Thermo-Fisher Scientific | Cat#A1049101 |
| Human AB-serum | Sigma | Cat#H4522 |
| Penicillin-Streptomycin | Thermo-Fisher Scientific | Cat#15140-122 |
| IMDM medium | Gibco | Cat#12440053 |
| DNAse I | Roche | Cat#10104159001 |
| Collagenase A | Roche | Cat#10103586001 |
| 100 μM cell strainers | BD Falcon | Cat#352360 |
| mouse α-human Fc-HRP | BioRad | Cat#MCA647P |
| PBS | Fresenius Kabi | Cat#1073508600 |
| Bovine serum albumin | Fisher Scientific | Cat#M090001/03 |
| TrueGuide$^{TM}$ Synthetic sgRNA | Thermo-Fisher Scientific | Cat#A35533 |
| Lymphoprep$^{TM}$ | Fresenius | Cat#AXI-1114547 |
| donkey anti-human IgG-HRP | Jackson ImmunoResearch | Cat#709-036-149 |
| human IFN-γ CBA flex set | BD Bioscience | Cat#560111 |
| Fc-receptor block | Miltenyi Biotec | Cat#130-059-901 |
| 7-Aminoactinomycin D | Sigma | Cat#A9400-1MG |
| 123counting eBeads | Thermo-Fisher Scientific | Cat#01-1234-42 |
| Antibody block | Discovery | Cat#760-4204 |
| ChromoMab DAB kit | Discovery | Cat#760-159 |
| hematoxylin II | Ventana | Cat#790-2208 |
| bluing reagent | Ventana | Cat#760-2037 |

## EXPERIMENTAL MODEL AND STUDY PARTICIPANT DETAILS

### Design, production, purification and humanization of bsTCEs

The following bsTCEs were generated: PSMA-Vδ2 bsTCE, Vδ2-PSMA bsTCE, humanized PSMA-Vδ2 bsTCE, humanized PSMA-Vδ2-Fc bsTCE, and control antibodies gp120-gp120-Fc bsTCE, gp120-Vδ2-Fc bsTCE and PSMA-gp120-Fc bsTCE (Figure S1 provides a schematic overview of the humanized PSMA-Vδ2 bsTCE and PSMA-Vδ2-Fc bsTCE). The control gp120-specific VHHL8CJ3 binds to glycoprotein (gp)120 of HIV-1.[61] The PSMA-Vδ2 and Vδ2-PSMA bsTCEs were constructed by linking the Vδ2-TCR-specific VHH5C8[28] and PSMA-specific VHHD2[27] using a 5 amino acid (a.a.) glycine (G)-serine (S) (sequence G4S) linker. Purified protein was produced by ImmunoPrecise antibodies (IPA, Utrecht, The Netherlands) using transient DNA transfection into HEK293E cells followed by purification using protein-A affinity chromatography (mAbSelect prismA) and preparative size exclusion chromatography using a Superdex 75 column.

The Vδ2-TCR-specific VHH5C8 and PSMA-specific VHHD2 were humanized using CDR grafting technology.[62] VHH sequences were aligned to the human germline[63] and the closest human germline VH segment was identified and used for direct grafting of the llama-derived CDR sequences. Next, the NCBI NR database was queried using BLASTP to identify human template sequences that demonstrated the highest identity to the llama-derived VHH sequences, preferentially with equal lengths of CDR loops and these were used for grafting of the llama-derived CDR sequences. To understand the effect of humanized framework residues on the structure of the VHHs, homology models were made using the 'Antibody Prediction'-tool (default parameters) within BioLuminate 4.2.156 (Schrödinger, LLC). The CDRs were grafted *in silico* to study the possible effect(s) of the human residues on features as loop conformation of the CDRs, the hydrophobicity of the surface and structural integrity (e.g., increased rigidity). The resulting constructs were checked for these features, resulting in the design of additional humanized sequences. All designed variants were expressed and purified as recombinant VHH proteins as described for PSMA-Vδ2 and Vδ2-PSMA. The PSMA-Vδ2-Fc bsTCE, gp120-gp120-Fc bsTCE, gp120-Vδ2-Fc bsTCE and PSMA-gp120-Fc consist of two polypeptide chains with the design: VHH-modified hinge-CH2-CH3. The two chains were designed to preferentially hetero-dimerize using knobs-into-holes (KIHs) technology[64] in CH3; the CH2 domains were silenced for Fc receptor interactions by the L234F and L235E (LFLE) mutations. In addition, a Cys220 deletion was included to avoid an unpaired cysteine and the hinge was slightly modified.[65] Expression and purification were performed as described above (co-transfection of two plasmids), except for the use of a Superdex-200 column instead of a Superdex-75. Purified proteins were found to be >95% pure (as judged by SDS-PAGE analysis) and >95% monomeric (as determined by HP-SEC analysis) and essentially free from endotoxins (0.05 EU/mg, as determined by a LAL assay).

### Tumor cell lines

LNCaP ($PSMA^+$ clone FGC, CRL-1740) and PC3 ($PSMA^-$, CRL-1435) were obtained from American Type Culture Collection (ATCC) and VCaP ($PSMA^+$, 06020201-1VL) and 22Rv1 ($PSMA^+$, 5092802) from the European Collection of Authenticated Cell Cultures (ECACC). Cell lines were maintained in Roswell Park Memorial Institute (RPMI) medium (22400089, Gibco) supplemented with 10% (v/v) fetal calf serum (FCS, 04-007-1A, Biological Industries), 0.05 mM β-mercaptoethanol (200-646-6, Merck), 100 IU/mL sodium penicillin, 100 μg/mL streptomycin sulfate and 2.0 mM L-glutamine (PSG, 10378-016, Life Technologies), referred to as RPMI complete medium. THP-1 cells were obtained from ECACC-Sigma (88081201) and cultured in RPMI 1640 ATCC modified medium (A10491-01, Thermo-Fisher Scientific) supplemented with 10% heat inactivated fetal bovine serum (FBS, SV30160.03, Cytiva), 0.5% gentamycin (15710-049, Gibco) and 5 mM β-mercaptoethanol (M6250, Sigma). Cell lines were kept at 37°C in a humidified atmosphere containing 5% $CO_2$ and tested for Mycoplasma using PCR every 3 months.

### Generation of LNCaP PSMA knock-out cell line

For the generation of a LNCaP-derived PSMA knock-out cell line, LNCaP cells were co-transfected with four predesigned synthetic CRISPR guide RNAs (CRISPR646020_SGM, CRISPR971863_SGM, CRISPR646032_SGM and CRISPR646028_SGM, Thermo-Fisher Scientific) and the recombinant *Streptococcus pyogenes* Cas9 (wt) protein (Thermo-Fisher Scientific) using Lipofectamine (Thermo-Fisher Scientific), according to manufacturer's recommendations (TrueGuide Synthetic sgRNA). Single cell clones were generated and PSMA expression was assessed using flow cytometry. Cells were kept at 37°C in a humidified atmosphere containing 5% $CO_2$.

### PBMC isolation and T cell cultures

Peripheral blood mononuclear cells (PBMC) derived from healthy donor- and PCa patient blood were isolated using Lymphoprep (AXI-1114547, Fresenius) density gradient centrifugation. Blood samples were obtained from Sanquin (Amsterdam, The Netherlands) in case of healthy donors or from PCa patients under written informed consent from the Amsterdam UMC (location VUmc, Amsterdam, The Netherlands). Patient characteristics can be found in Table S1. PBMC were processed for phenotypic analysis using flow cytometry or resuspended in RPMI medium complete for functional experiments.

Healthy donor-derived Vγ9Vδ2 T cells were isolated from PBMC and expanded as described before.[45] In short, Vγ9Vδ2 T cells were isolated from PBMC using magnetic bead sorting with FITC-labeled Vδ2 monoclonal antibodies (mAbs, Table S2) in combination with anti-mouse IgG microbeads (130-048-401, Miltenyi). Purified Vγ9Vδ2 T cells were stimulated weekly with irradiated feeder mix consisting of healthy donor PBMC ($1x10^6$ cells/ml), JY cells ($1x10^5$ cells/mL, 94022533, ECACC), IL-7 (10 U/mL, 207-IL-025, R&D

Systems), IL-15 (10 ng/mL, 34-8159-85, eBioscience), and PHA (50 ng/mL, R30852801, Thermo Fisher Scientific) and used in experiments if purity of Vγ9Vδ2 T cells was >95% of total cells (referred to as expanded Vγ9Vδ2 T cells). Alternatively, Vγ9Vδ2 T cells were isolated from PBMC using the EasySep human gamma/delta T cell negative isolation kit (19255, STEMCELL Technologies) and directly used in functional experiments (referred to as non-expanded Vγ9Vδ2 T cells).

M1-specific and pp65-specific $CD8^+$ T cells were isolated from PBMC of $CMV^+$ and $influenza^+$ experienced donors (Sanquin) using an enrichment step (EasySep human $CD8^+$ T cell isolation kit, 17953, STEMCELL Technologies) and subsequent sorting of $CD8^+$ T cells using a BV510 labeled CD8α antibody (Table S2) and the A*02:01-GILGFVFTL-dextramer (WB2161-APC, Immudex) for M1-specific $CD8^+$ T cells or the A*02:01-NLVPMVATV-dextramer (WB2132-APC, Immudex) for pp65-specific $CD8^+$ T cells. Cells were expanded using a rapid expansion protocol by culturing the cells in the presence of irradiated (5000 rad) allogeneic PBMC (mixed from 3 donors) and irradiated (5000 rad) JY cells in T cell medium consisting of 50% CTS AIM-V Medium (A3830801, Thermo-Fisher Scientific) and 50% RPMI 1640 medium (A1049101, Thermo-Fisher) supplemented with 10% heat inactivated human AB-serum (H4522, Sigma) and 1% Penicillin-Streptomycin (15140-122, Thermo-Fisher Scientific) in the presence of 30 ng/mL anti-CD3 antibody (OKT3, 16-0037-81, Thermo-Fisher Scientific) and 3000 IU/mL IL-2 (130-097-748, Miltenyi Biotec). After the initial 7 days of culture, medium was replaced every 2 days with fresh T cell medium supplemented with 3000 IU/mL IL-2, but on day 16 a lower concentration of IL-2 (60 IU/mL) was added. Cells were cryopreserved 3–5 days later and thawed when needed for functional experiments. After thawing, $CD8^+$ T cells were expanded in T cell medium supplemented with irradiated (5000 rad) allogeneic PBMC (mixed from 3 donors) and irradiated (5000 rad) JY cells, 50 ng/mL PHA, 250 IU/mL IL-2 and 10 ng/mL IL-15 (130-095-766, Miltenyi Biotec) and used in the assays at least 7 days after the last addition of cytokines. MART-1 specific $CD8^+$ T cells were generated[66] and expanded as described for M1-and pp65-specific $CD8^+$ T cells (above) with the addition of pre-loading JY cells with 1 μM MART-1 short peptide (SP, ELAGIGILTV, custom, ProImmune) to promote expansion of ELAGIGILTV-specific $CD8^+$ T cells. Vγ9Vδ2 T cell and $CD8^+$ T cell donors were HLA-A2 matched.

All T cell cultures were kept at 37°C in a humidified atmosphere containing 5% $CO_2$.

### PCa patient tissue samples

Non-malignant and malignant tissue samples were collected from radical prostatectomies of patients with non-metastatic prostate cancer at the Amsterdam UMC (location VUmc) after written informed consent (characteristics of 39 patients can be found in Table S1, ethical approval number: U2017-013). The pathologist assessed whether the tissue pieces were of non-malignant or malignant origin by macroscopic analysis in combination with clinical and radiological findings provided by treating physicians. Tissues were cut into small pieces, resuspended in dissociation medium composed of Iscove's Modified Dulbecco's Medium (IMDM, 12440053, Gibco) supplemented with 0.1% DNAse I (10104159001, Roche), 0.14% Collagenase A (10103586001, Roche), PSG and 5% FCS, transferred to a sterile flask and incubated on a magnetic stirrer for 45 min at 37°C. Subsequently, cell suspensions were run through a 100 μM cell strainer (352360, BD Falcon). Dissociation steps were repeated 1–3 rounds in total from incubation in dissociation medium onwards. Single cell suspensions derived from these tissues were processed for phenotypic analysis using flow cytometry and/or resuspended in RPMI complete medium for functional testing depending on the available cell quantity.

### *In vivo* tumor rejection

An *in vivo* anti-tumor efficacy study was performed by Crown Bioscience (Taichang, China) according to the Institutional Animal Care and Use Committee (IACUC)-approved protocol and in accordance with the regulations of the Association for Assessment and Accreditation of Laboratory Animal Care (AAALAC) (ethical approval number: AN-2004-12-1378). Female immunodeficient NCG mice (the NOD/ShiLtJGpt-Prkdcem26Cd52Il2rgem26Cd22/Gpt strain, 6–8 weeks old) were subcutaneously inoculated with $5x10^6$ 22Rv1 $PSMA^+$ tumor cells admixed with PBMC of either of two human healthy donors (Vγ9Vδ2 T cell percentages of $CD3^+$ cells: 21.9% and 8.8%), in a 2:1 22Rv1:PBMC ratio. After tumor cell-PBMC inoculation ($n$ = 4 or $n$ = 12 per group), PBS (vehicle control) or PSMA-Vδ2-Fc bsTCE (at doses of 0.2 and 2.0 mg/kg) were intravenously administered weekly (day 0, 7, 14 and 21). Tumor volumes were measured twice per week using a caliper, and the volume was expressed in $mm^3$ using the formula: "V = (L x W x W)/2, where V was tumor volume, L was tumor length (the longest tumor dimension) and W was tumor width (the longest tumor dimension perpendicular to L). At the end of the follow-up period tumor growth inhibition (TGI) in percentage was calculated as: ((tumor volume of PSMA-Vδ2 bsTCE treated mice in $mm^3$ – tumor volume of PBMC treated mice in $mm^3$)/tumor volume of PBMC treated mice in $mm^3$)* 100%. Mice were sacrificed when the mean tumor volume of a group exceeded 2000 $mm^3$.

### *In vivo* pharmacokinetics of the PSMA-Vδ2-Fc bsTCE

Pharmacokinetic (PK) characteristics of PSMA-Vδ2-Fc bsTCE were assessed in two *in vivo* studies. The first study was performed in human neonatal Fc receptor (hFcRn) expressing mice by The Jackson Laboratory (Bar Harbor, USA) according to an American Association for Laboratory Animal Science (IACUC)-approved protocol and in compliance with the Guide for the Care and Use of Laboratory Animals (National Research Council, 1996) (ethical approval number: 15006-A78). Male Tg32 SCID mice (the B6.Cg-$Fcgrt^{tm1Dcr}$ $Prkdc^{scid}$ Tg[FCGRT]32DcrJ strain, 7–10 weeks old) expressing human FcRn received PSMA-Vδ2-Fc bsTCE and trastuzumab (as a reference IgG1 antibody) co-administered intravenously at 2, 5 or 10 mg/kg ($n$ = 4 per dose). One group of mice received PSMA-Vδ2-Fc (5 mg/kg) alone to rule out any potential effect that trastuzumab could have on the PK of PSMA-Vδ2-Fc bsTCE. Blood samples were collected at different time points (5 min, 8h and 1, 3, 7, 10, 14, 17, 21 and 28 days) after compound administration, and

concentrations of PSMA-Vδ2-Fc bsTCE or trastuzumab were determined using an antigen capture ELISA (Lava Therapeutics, Utrecht, The Netherlands); plates were coated O/N with human PSMA protein (1 μg/mL) and PSMA-Vδ2-Fc bsTCE detection was performed using monoRab rabbit anti-camelid VHH-HRP conjugate (clone 96A3F5, A01861-200, Genscript). An anti-idiotype ELISA was used for trastuzumab quantification; plates were coated O/N with mouse anti-trastuzumab antibody (clone AbD18018, HCA168, BioRad) and trastuzumab antibody detection was assessed by mouse α-human Fc-HRP (MCA647P, BioRad). Toxicokinetic parameters can be found in Table S3.

The second study was performed in non-human primates (NHP), whose FcRn is highly homologous to human FcRn, by Covance Laboratories Limited (Cambridgeshire, UK) in accordance with the applicable sections of the United Kingdom Animals (Scientific Procedures) Act 1986, Amendment Regulations 2012 (the Act) (ethical approval number: P8A1A5297). In this study, PK parameters were assessed in three female *Macaca fascicularis* (2.12–2.18 kg, 29–31 months old) that were intravenously injected with a single dose of 0.03, 1.0 or 3.0 mg/kg PSMA-Vδ2-Fc bsTCE ($n$ = 1/dose). Venous blood samples were collected at different timepoints (30 min, 1, 2, 4, 8h and 1, 3, 5, 7, 14, 21 and 22 days) after compound administration and PSMA-Vδ2-Fc bsTCE concentrations in plasma were determined using a free drug assay (at Lava Therapeutics). Microtiter plate wells were coated with 2.5 μg/mL PSMA protein (15877-H07H, Sino Biological) and HRP labeled-rabbit anti-camelid VHH-antibody (A011861, Genscript) was used for detection. Toxicokinetic parameters can be found in Table S4.

## METHOD DETAILS

### Flow cytometry

Cells were resuspended in PBS (1073508600, Fresenius Kabi) supplemented with 0.5% bovine serum albumin (M090001/03, Fisher Scientific) and 20 μg/mL $NaN_3$ (247-852-1, Merck) and incubated with fluorochrome-labeled antibodies (Abs, Table S2) for 30 min at 4°C. Unbound fluorochrome-labeled Abs were washed away. The LSR Fortessa XL-20 (BD) was used for data-acquisition and flow cytometry data were analyzed using Kaluza Analysis Version 1.3 (Beckman Coulter) or FlowJo Version 10.6.1 and 10.7.2 (Becton Dickinson). Cytometric Bead Array (CBA) data were analyzed with FCAP Array software v3.0 (BD).

### Assessment of target specificity and binding characteristics of bsTCEs

Binding of bsTCEs or control bsTCE to the Vδ2 chain of the Vγ9Vδ2-TCR and to PSMA was determined as follows: Vγ9Vδ2 T cells were incubated with different concentrations of bsTCE or control bsTCE, and after unbound bsTCE was washed away, bound bsTCE was detected with FITC-labeled anti-llama polyclonal Ab or AF647-labeled anti-VHH (Table S2) after which cells were analyzed using flow cytometry. Binding of bsTCEs to LNCaP and PC3 tumor cells was detected using a whole cell ELISA. Tumor cells were plated in 96-well cell culture plates and 48h later incubated with different concentrations of bsTCE. Bound bsTCE was detected using rabbit anti-camelid VHH cocktail (19L002038, GenScript) or donkey anti-human IgG-HRP (709-036-149, Jackson ImmunoResearch) and 3, 3′, 5, 5′-tetramethylbenzidine (TMB) was used as a substrate for color development. The absorbance (450 nm) was measured using a plate reader (Molecular Devices, iD5) and data were analyzed using SoftMax Pro software v7.1 (Molecular Devices).

### Assessment of Vγ9Vδ2 T cell activation

The capacity of PSMA-Vδ2 bsTCEs to induce Vγ9Vδ2 T cell activation was assessed using different sources of Vγ9Vδ2 T cells. Expanded healthy donor-derived Vγ9Vδ2 T cells were incubated with LNCaP (WT or PSMA knock-out), PC3, 22Rv1 or VCaP tumor cells (1:1 E:T ratio) and different concentrations of the bsTCEs or control bsTCEs; prostate cancer patient PBMC were incubated with autologous prostate cancer patient dissociated tissue suspensions (10:1 E:T ratio) and different concentrations of the bsTCEs. In parallel, prostate cancer patient dissociated tissue suspensions (containing infiltrated Vγ9Vδ2 T cells) were incubated with different concentrations of bsTCEs. PE-labeled CD107a mAb was added during incubation to allow evaluation of degranulation. After 24 h Vγ9Vδ2 T cell degranulation and CD25 expression was assessed, and culture supernatants were collected and stored at −20°C until analysis using the human IFN-γ CBA flex set (560111, BD Bioscience). For blocking experiments, Vγ9Vδ2 T cells or prostate cancer patient dissociated tissue suspensions were incubated 30 min with 10 μg/mL Fc-receptor block (130-059-901, Miltenyi Biotec) followed by a 30 min incubation with DNAM-1 (clone DX11, 559787, BD Bioscience), NKG2D (clone 149810, MAB139–100, R&D Systems), NKG2A (monalizumab, PX-TA1392-100UG, Proteogenics) blocking antibodies or IgG1 isotype control antibody (MAB002, R&D Systems) before incubation with bsTCEs. LNCaP, VCaP or 22Rv1 cells were incubated for 30 min with BTN3A (clone 103.2, PABL-415, Creative Biolabs) blocking antibodies.

### Assessment of target cell lysis

Lysis of target cells was assessed by incubating expanded healthy donor-derived Vγ9Vδ2 T cells with prostate tumor cells (LNCaP, PC3, 22Rv1 or VCaP) or prostate cancer patient dissociated tissue suspensions (1:1 E:T ratio) in the presence of the bsTCE or control bsTCEs for 24h or by incubating prostate cancer patient PBMC with autologous prostate cancer patient dissociated tissue suspensions (10:1 E:T ratio) in the presence of the bsTCE (50 nM) for 24h. Tumor lysis was determined using 7-Aminoactinomycin D (7AAD, A9400-1MG, Sigma) and 123counting eBeads (01-1234-42, Thermo-Fisher) followed by flow cytometric analysis. Percentages of lysis were calculated based on cell numbers relative to target cell only or to target cell + Vγ9Vδ2 T cell conditions.

### Assessment of APC function of Vγ9Vδ2 T cells

Different experiments were performed to study the capacity of the bsTCE to promote antigen presentation by Vγ9Vδ2 T cells. Vγ9Vδ2 T cells were incubated on PSMA-coated plates (1 μg/mL, 2h pre-incubation at room temperature, 15877-H07H, Sino Biologicals) and either medium control or 10 p.m. PSMA-Vδ2 bsTCE to induce TCR-mediated activation. After 24h incubation, expression of APC-associated molecules CD83, HLA-A2 and HLA-DR (Table S2) by Vγ9Vδ2 T cells (non-expanded) was assessed using flow cytometry. Cross-presentation of virus-specific or tumor-associated antigens by bsTCE-activated Vγ9Vδ2 T cells to $CD8^+$ T cells was assessed by analysis of the activation state of the $CD8^+$ T cells after co-culture of bsTCE-activated Vγ9Vδ2 T cells and peptide-specific $CD8^+$ T cells. As the $CD8^+$ T cells recognize their target peptide in the context of HLA-A2, Vγ9Vδ2 T cells from HLA-A2 positive donors were used in these experiments. Expanded or non-expanded Vγ9Vδ2 T cells were pre-incubated for 24h on PSMA-coated wells with 0 or 10 p.m. PSMA-Vδ2 bsTCE in the presence or absence of 1 μM long peptides (LP) M1 (30-mer, influenza-derived antigen, LKTRPILSPLTKGILGFVFTLTVPSERGLQ), MART-1 (25-mer, tumor-associated antigen, GHGHSYTTAEELAGIGILTVILGVL) or pp65 (30-mer, CMV-derived antigen, TWPPWQAGILARNLVPMVATVQGQNLKYQE) which were custom made by ProImmune. Vγ9Vδ2 T cells (expanded) pre-treated with the M1 or MART-1 LPs, were subsequently co-cultured for 16-24h with M1-or MART-1-specific $CD8^+$ T cells; Vγ9Vδ2 T cells (non-expanded) pre-treated with pp65 LP, were co-cultured with pp65-specific $CD8^+$ T cells. Percentages of CD69, CD25, CD107a and IFN-γ (Table S2) positive $CD8^+$ T cells were determined using flow cytometry. In some experiments, Vγ9Vδ2 T cells (expanded) that were pre-treated with pp65 LP were subsequently co-cultured for 7 days with $CD8^+$ T cells, which were negatively isolated from a CMV positive donor to determine proliferation of $pp65^+$ $CD8^+$ cells within the $CD8^+$ population. Unloaded or pp65 short peptide (SP, NLVPMVATV, custom, ProImmune)-loaded THP-1 tumor cells were added as target cells to the 7-day culture conditions to analyze tumor cytotoxicity using flow cytometry.

### Tissue-cross reactivity

To explore human tissue reactivity, the PSMA-Vδ2-Fc bsTCE was FITC-labeled by Squarix GmbH (Marl, Germany) using a controlled reaction with NHS-coupled FITC. The average number of fluorochrome molecules conjugated per protein (F/P) was 4.3. Tissue-reactivity was assessed by Charles River Laboratories (Evreux, France) through immunohistochemistry (IHC) technique using the FITC-labeled PSMA-Vδ2 bsTCE on a panel of 41 different frozen normal human tissues (adrenal, bone marrow, breast/mammary gland, cecum, cerebellum, cerebral cortex, colon, duodenum, endothelium [vessels], eye, esophagus, fallopian tube [oviduct], gall bladder, heart [ventricle], ileum, jejunum, kidney [cortex], liver, lung, lymph node, muscle [striated, skeletal], peripheral nerve, ovary, pancreas, parotid, parathyroid pituitary, placenta, prostate, rectum, skin, spinal cord, spleen, stomach, testis, thymus, thyroid, tonsil, ureter, urinary bladder, uterus [cervix] and uterus [endometrium]) and peripheral blood smears (three donors per tissue or blood smear). Frozen sections were air-dried, fixed in zinc formalin (4087236, Microm Microtech) and rinsed using Milipore water. Test tissue samples were incubated with 0, 3 or 20 μg/mL FITC-labeled PSMA-Vδ2-Fc bsTCE followed by 2 μg/mL HRP-conjugated goat α-FITC antibody (01-40-01, KPL) after which antibody block (760–4204, Discovery) was applied. The ChromoMab DAB kit (760-159, Discovery) was used for detection according to the manufacturer's recommendations. Test samples were then stained with hematoxylin II (790–2208, Ventana) and bluing reagent (760–2037, Ventana), washed, dehydrated and mounted. Slides were evaluated by a pathologist using a light microscope (Olympus BX51).

## QUANTIFICATION AND STATISTICAL ANALYSIS

GraphPad Prism v9.1.0 (GraphPad Software) was used for statistical analyses. Data were analyzed using paired or unpaired t test, one-way ANOVA with Dunnet multiple comparisons test or Mantel–Cox test or two-way ANOVA with Tukey test as appropriate. $p < 0.05$ was considered significant and indicated with asterisks: $p < 0.05$: *, $p < 0.01$: **, $p < 0.001$: *** and $p < 0.0001$: ****. $EC_{50}$ values were calculated using nonlinear regression analysis with GraphPad Software.